

SUPPLEMENTARY INFORMATION

C-functionalized chiral dioxocyclam and cyclam derivatives with 1,2,3-triazole units: synthesis, complexation properties and crystal structure of copper(II)-complexes

Anne-Sophie Felten, Nicolas Petry, Bernard Henry, Nadia Pellegrini-Moïse*, Katalin Selmeczi*

Figure S1. X-ray structure of $[\text{Cu}(\text{syn-25})]$ complex.

Figure S2. Visible absorption spectra of the complex $[\text{Cu}(\text{anti-23})]$ in H_2O at different pH.

Figure S3. Visible CD spectra of the complex $[\text{Cu}(\text{anti-23})]$ in H_2O at different pH.

Figure S4. A) ESI-MS spectrum (mode positive) of copper(II) complex of *anti-23*. B) Molecular ion peaks of complex between 500 and 650 m/z values with observed (B) and simulated (C) isotopic distribution for $[\text{C}_{23}\text{H}_{31}\text{N}_{10}\text{O}_2\text{Cu}]^+$ ($[\text{M}+\text{H}]^+$), $z = 1$.

Figure S5. A) ESI-MS spectrum (mode positive) of copper(II) complex of *anti-27*. B) Molecular ion peaks of complex between 500 and 650 m/z values with observed (B) and simulated (C and D) isotopic distribution for $[\text{C}_{23}\text{H}_{36}\text{N}_{10}\text{CuCl}]^+$ ($[\text{M}+\text{Cl}]^+$) and $[\text{C}_{23}\text{H}_{35}\text{N}_{10}\text{Cu}]^+$ ($[\text{M}-\text{H}]^+$), $z = 1$.

Figure S6. A) ESI-MS spectrum (mode positive) of copper(II) complex of *anti-27*. B) Molecular ion peaks of complex between 250 and 350 m/z values with observed (B) and simulated (C) isotopic distribution for $[\text{C}_{23}\text{H}_{36}\text{N}_{10}\text{Cu}]^{2+}$ ($[\text{M}]^{2+}$), $z = 2$.

Figure S7. Visible CD spectra of the complexes $[\text{Cu}(\text{anti-27})]^{2+}$ and $[\text{Cu}(\text{syn-28})]^{2+}$ in H_2O at different pH between 2 and 11. [complex] = 5 mM, $T = 298$ K.

Figure S8. Visible absorption spectra of the complex $[\text{Cu}(\text{anti-27})]^{2+}$ in H_2O at different pH between 2 and 11. [complex] = 5 mM, $T = 298$ K.

Figure S9. Measured CD spectra of the complex $[\text{Cu}(\text{anti-27})]^{2+}$ in H_2O at different pH between 2 and 11. [complex] = 5 mM, $T = 298$ K.

Figure S10. Visible absorption spectra of the complex $[\text{Cu}(\text{anti-27})]^{2+}$ in aqueous ammonium acetate buffer at pH = 6.5 measured from 0 to 10 sec every 0.5 sec.

Figure S11. Time course of the copper(II) complexation by *anti-27* ligand in aqueous ammonium acetate buffer. A) Absorbance at 530 nm of $[\text{Cu}(\text{anti-27})]^{2+}$ complex. B) % Cu(II) complexation.

Figure S12. Visible absorption spectra of the complex $[\text{Cu}(\text{anti-27})]^{2+}$ in 5 M HCl solution at 50°C over time at 0, 3.5, 20.5, 44, 96 and 720 hours.

Figure S13. Fitting of experimental data at 530 nm with exponential curve of pseudo first order kinetic by the program Berkeley Madonna 8.3.18.

Table S1. Crystal data and X-ray experimental parameters for $[\text{Cu}(\text{syn-25})]$.

Table S2. Values of Absorbance at 530 nm of $[\text{Cu}(\text{anti-27})]^{2+}$ complex and % Cu(II) complexation during the time course of the copper(II) complexation by *anti*-**27** ligand in aqueous ammonium acetate buffer. $[\text{anti-27}] = [\text{Cu}^{2+}] = 5 \text{ mM}$, $T = 298 \text{ K}$, $\text{pH} = 6.5$.

Characterization of compounds 1b-6b

Copies of ^1H and ^{13}C NMR spectra for compounds 1-30

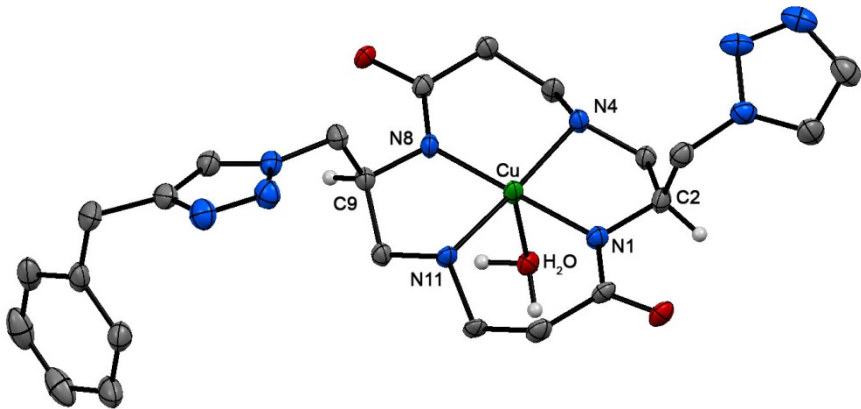


Figure S1. ORTEP diagram of $[\text{Cu}(\text{syn-25})]$ complex with thermal ellipsoids at 50 % probability. H-atoms have been omitted for clarity except on C2 and C9 atoms. Bond lengths and bond angles around the metal ion: N1 – Cu 1.958 Å, N4 – Cu 2.016 Å, N8 – Cu 1.960 Å, N11 – Cu 2.008 Å, H₂O – Cu 2.627 Å, N1 – Cu – N11 95.33°, N11 – Cu – N8 84.95°, N8 – Cu – N4 94.52°, N4 – Cu – N1 85.16°, N1 – Cu – OH₂ 88.04°.

Table S1. Crystal data and X-ray experimental parameters for $[\text{Cu}(\text{syn-25})]$.

Compound reference	$[\text{Cu}(\text{syn-25})]$
Chemical formula	C ₂₃ H ₃₄ CuN ₁₀ O ₄ ·2H ₂ O
Formula Mass	578.14
Crystal system	Tetragonal
a/Å	12.25040(10)
b/Å	12.25040(10)
c/Å	42.3729(7)
α/°	90
β/°	90
γ/°	90
Unit cell volume/Å ³	6359.00(15)
Temperature/K	100(2)
Space group	P4 ₃ 2 ₁ 2
No. of formula units per unit cell, Z	8
Radiation type	CuK α
Absorption coefficient, μ/mm^{-1}	1.322
No. of reflections measured	89613
No. of independent reflections	6691
R_{int}	0.0796
Final R_I values ($I > 2\sigma(I)$)	0.0438
Final $wR(F^2)$ values ($I > 2\sigma(I)$)	0.1061
Final R_I values (all data)	0.0463
Final $wR(F^2)$ values (all data)	0.1083
Goodness of fit on F^2	1.043
Flack parameter	-0.004(11)
CCDC deposit number	1435292

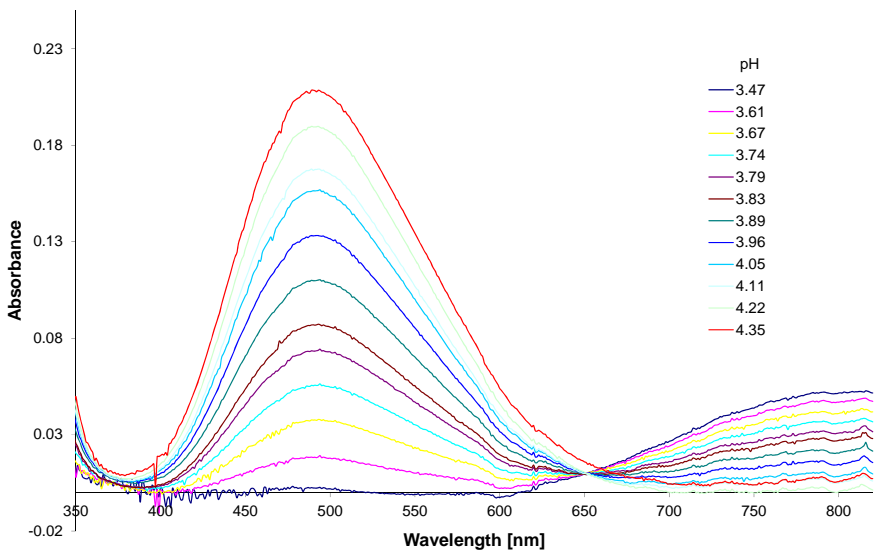


Figure S2. Visible absorption spectra of the complex $[\text{Cu}(\text{anti-23})]$ in H_2O at different pH.

[complex] = 5 mM, $T = 298$ K, at pH 4.35 precipitation of the complex was started.

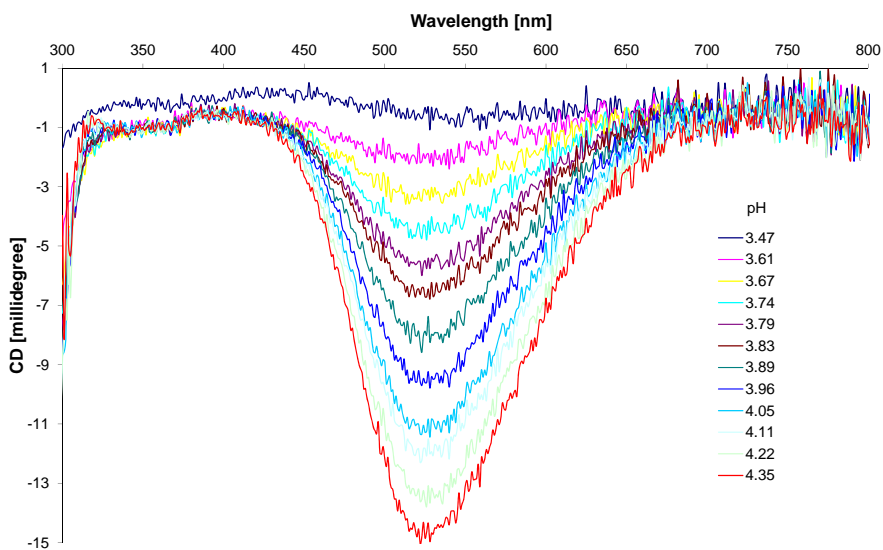


Figure S3. Visible CD spectra of the complex $[\text{Cu}(\text{anti-23})]$ in H_2O at different pH.

[complex] = 5 mM, $T = 298$ K, at pH 4.35 precipitation of the complex was started.

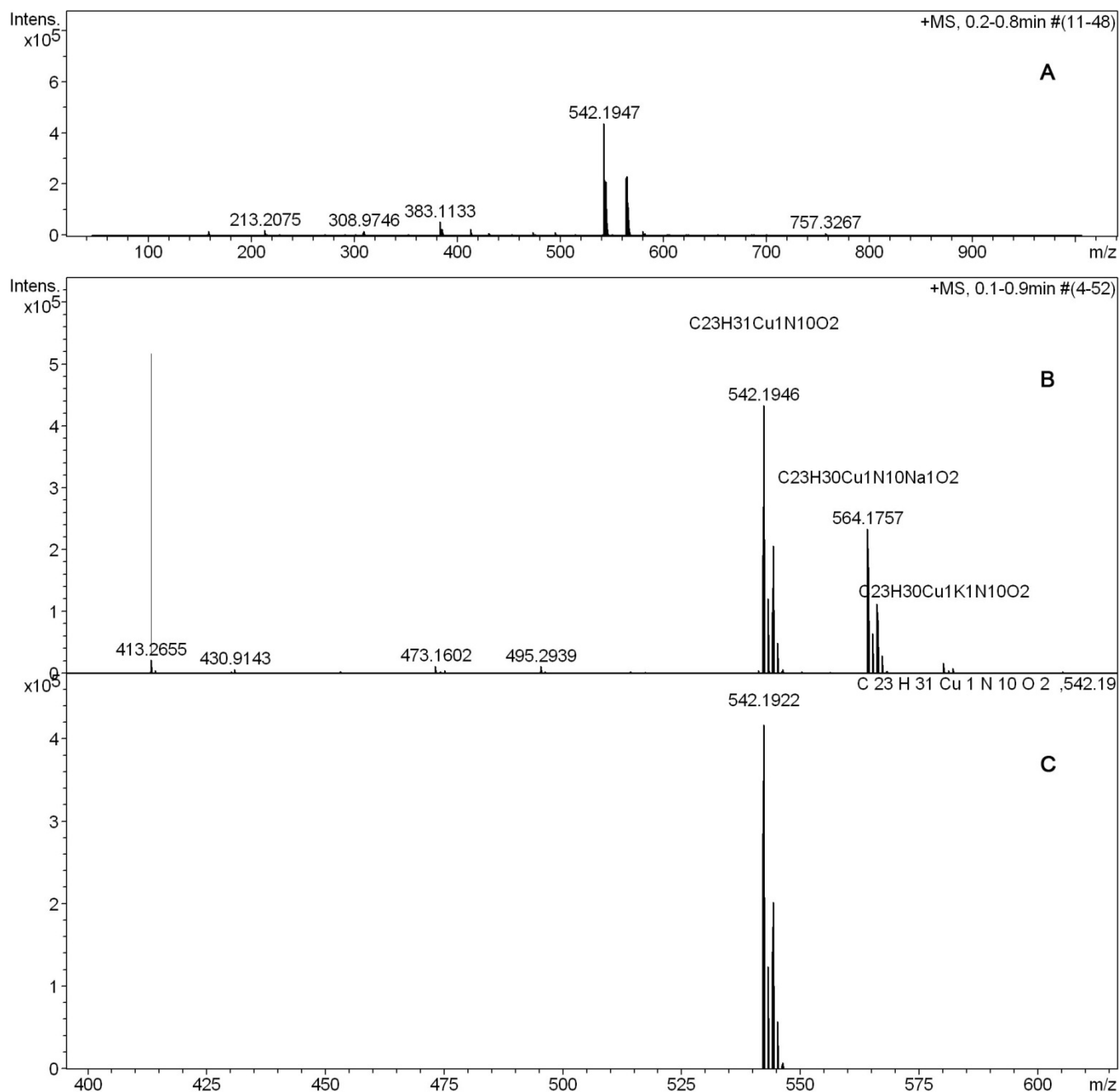


Figure S4. A) ESI-MS spectrum (mode positive) of copper(II) complex of *anti*-**23**. B) Molecular ion peaks of complex between 500 and 650 m/z values with observed (B) and simulated (C) isotopic distribution for $[C_{23}H_{31}N_{10}O_2Cu]^{+}$ ($[M+H]^{+}$), $z = 1$.

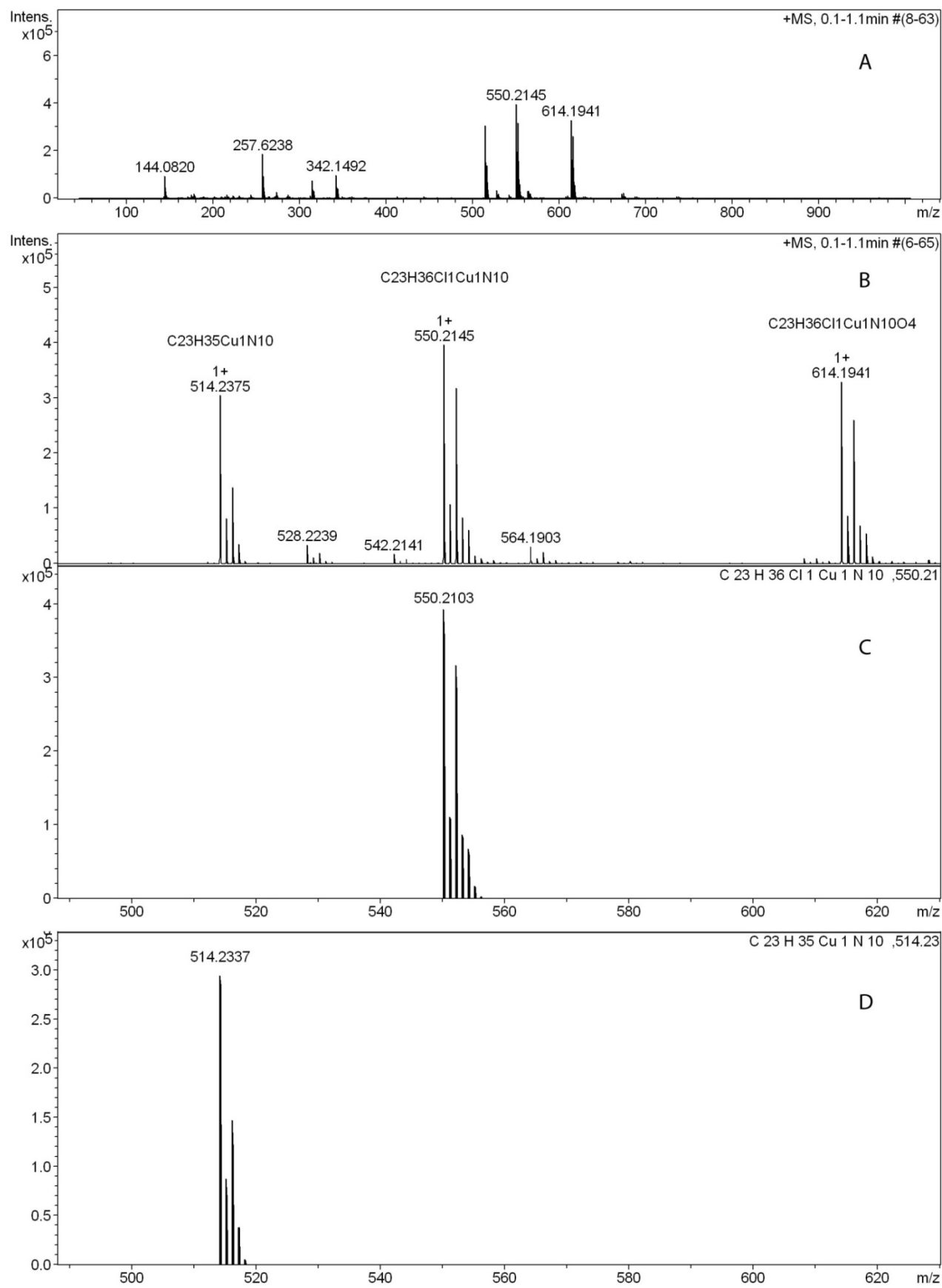
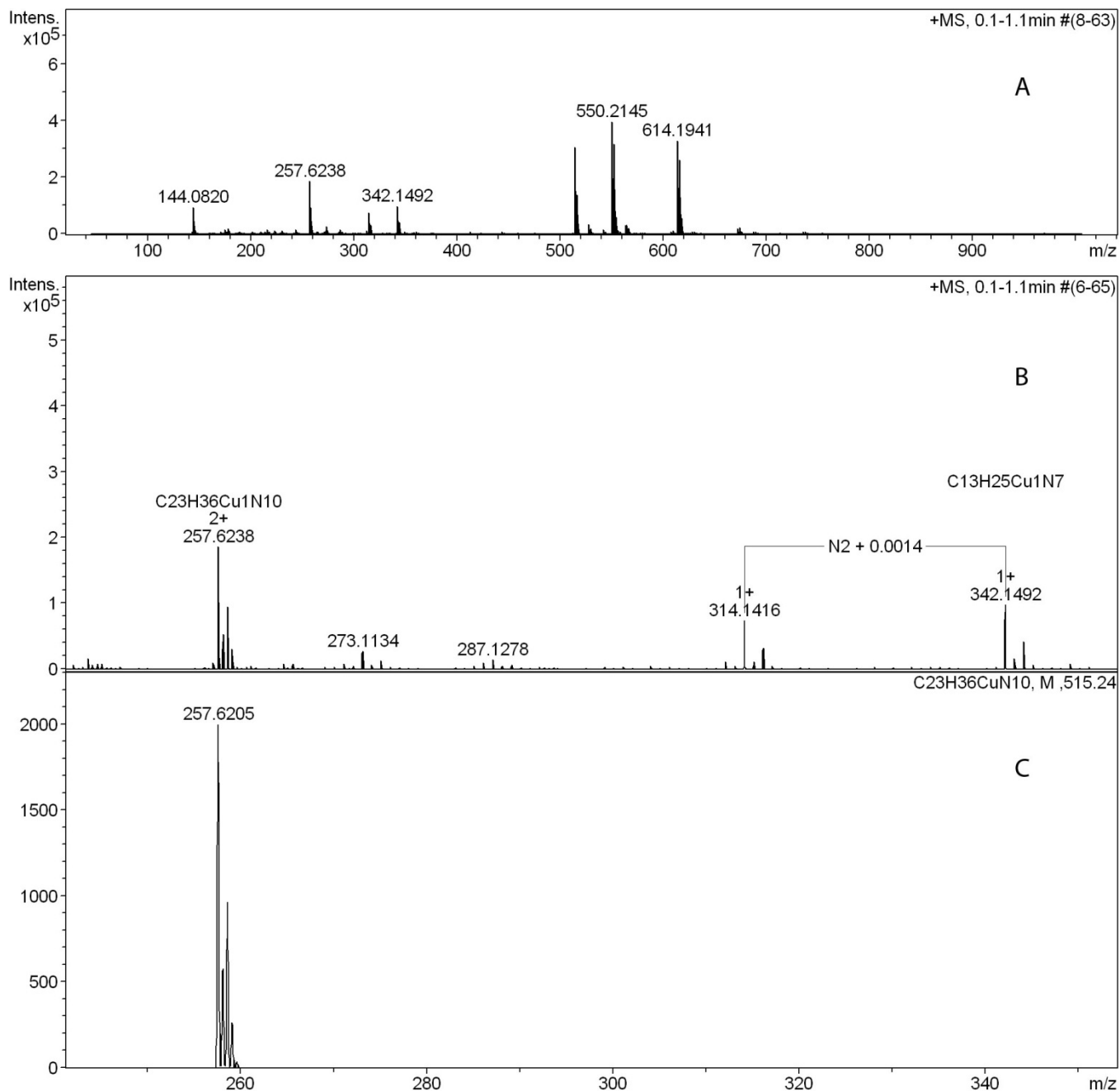


Figure S5. A) ESI-MS spectrum (mode positive) of copper(II) complex of *anti*-27. B) Molecular ion peaks of complex between 500 and 650 m/z values with observed (B) and simulated (C and D) isotopic distribution for $[C_{23}H_{36}N_{10}CuCl]^{+}$ ($[M+Cl]^{+}$) and $[C_{23}H_{35}N_{10}Cu]^{+}$ ($[M-H]^{+}$), $z = 1$.



Meas. m/z	#	Formula	m/z	err [mDa]	err [ppm]	mSigma	rdb	e ⁻ Conf	N-Rule
257.6238	1	C ₂₃ H ₃₆ CuN ₁₀	257.6205	-3.3	-12.8	17.2	10.5	odd	ok
342.1492	1	C ₁₃ H ₂₅ CuN ₇	342.1462	-3.0	-8.7	12.3	4.5	even	ok
514.2375	1	C ₂₃ H ₃₅ CuN ₁₀	514.2337	-3.9	-7.5	18.3	11.0	odd	ok
550.2145	1	C ₂₃ H ₃₆ ClCuN ₁₀	550.2103	-4.2	-7.6	11.7	10.0	odd	ok
614.1941	1	C ₂₃ H ₃₆ ClCuN ₁₀ O ₄	614.1900	-4.1	-6.6	16.8	10.0	odd	ok

Figure S6. A) ESI-MS spectrum (mode positive) of copper(II) complex of *anti*-27. B) Molecular ion peaks of complex between 250 and 350 m/z values with observed (B) and simulated (C) isotopic distribution for $[C_{23}H_{36}N_{10}Cu]^{2+}$ ($[M]^{2+}$), $z = 2$.

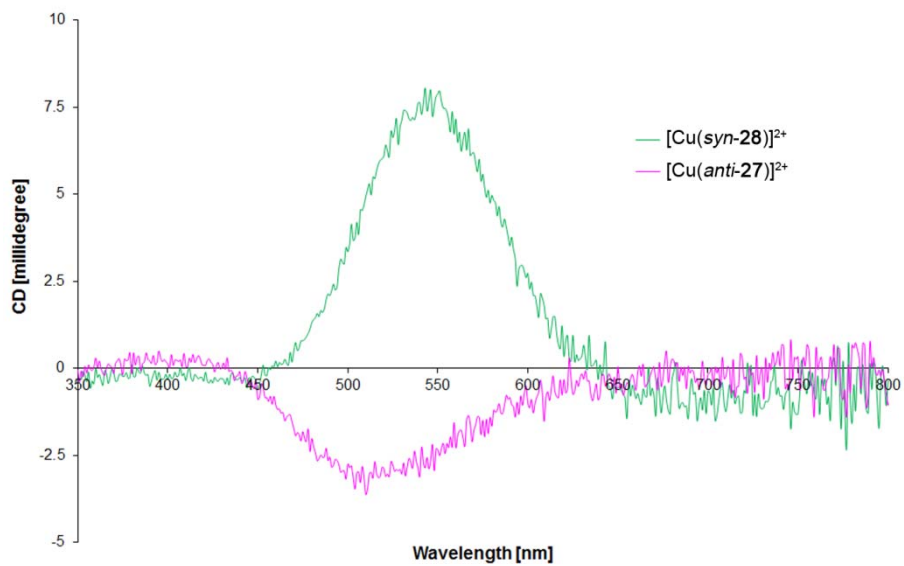


Figure S7. Visible CD spectra of the complexes $[\text{Cu}(\text{anti-27})]^{2+}$ and $[\text{Cu}(\text{syn-28})]^{2+}$ in H_2O at different pH between 2 and 11. [complex] = 5 mM, T = 298 K.

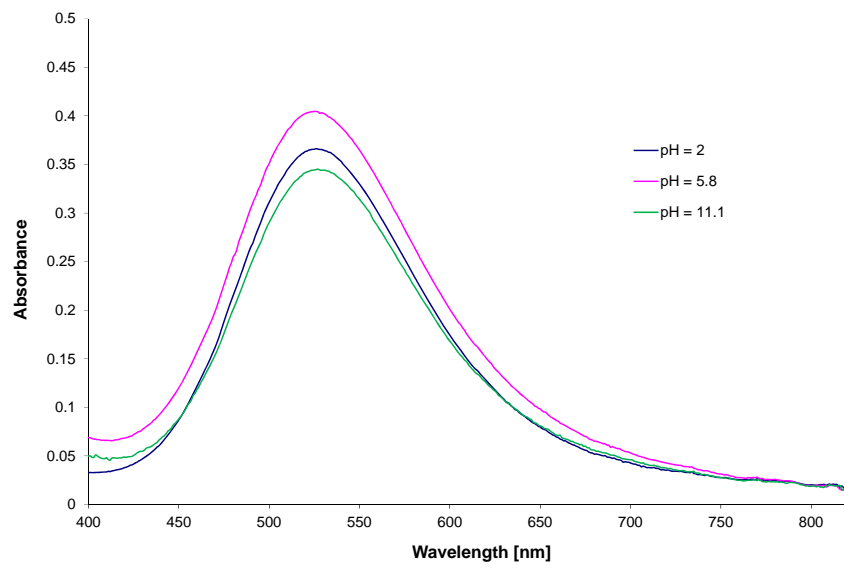


Figure S8. Visible absorption spectra of the complex $[\text{Cu}(\text{anti-27})]^{2+}$ in H_2O at different pH between 2 and 11. [complex] = 5 mM, $T = 298$ K. Change of intensity is due to the dilution after addition of HCl and NaOH solution for pH adjustment.

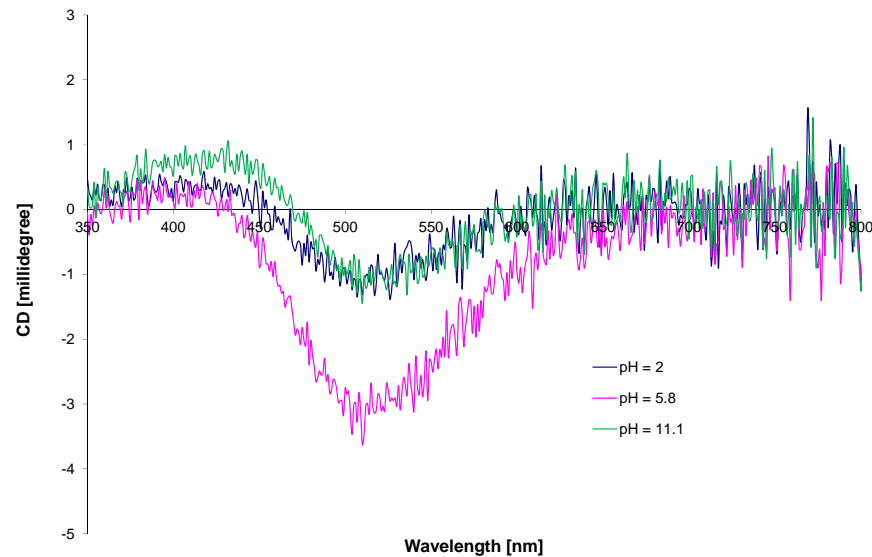


Figure S9. Measured CD spectra of the complex $[\text{Cu}(\text{anti-27})]^{2+}$ in H_2O at different pH between 2 and 11. [complex] = 5 mM, $T = 298$ K. Change of intensity is due to the dilution after addition of HCl and NaOH solution for pH adjustment.

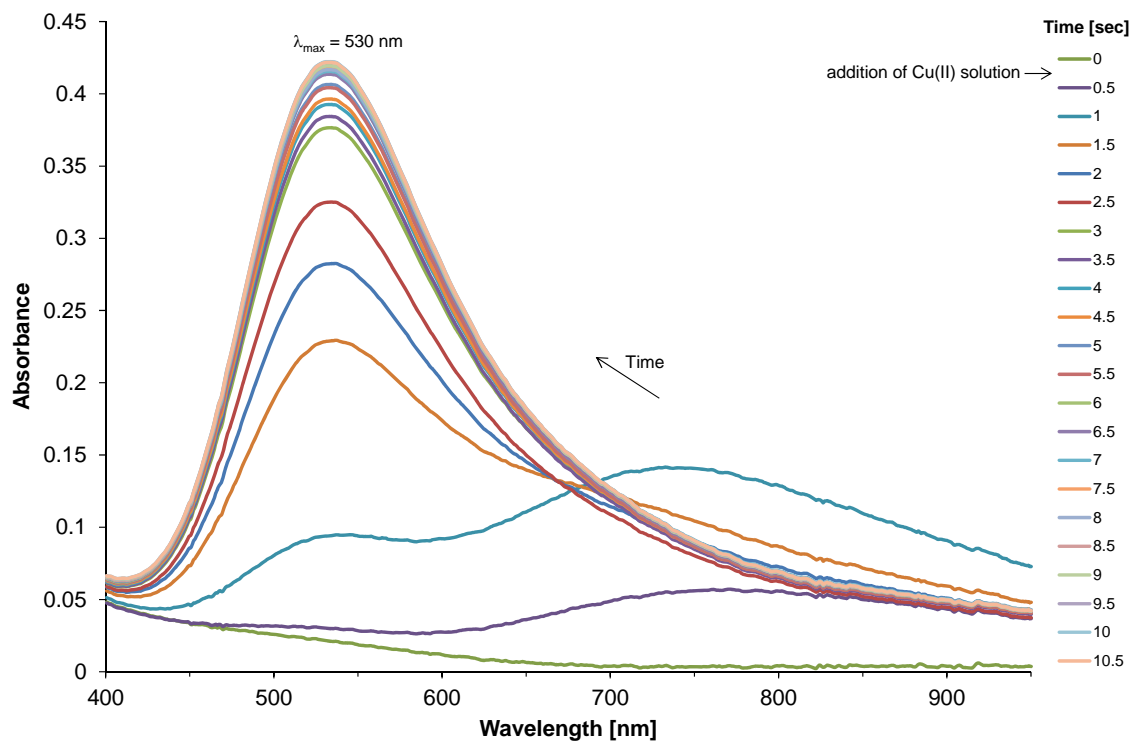


Figure S10. Visible absorption spectra of the complex $[\text{Cu}(\text{anti-27})]^{2+}$ in aqueous ammonium acetate buffer at $\text{pH} = 6.5$ measured from 0 to 10 sec, every 0.5 sec. Only one species seems to be formed as shown by the λ_{\max} of d-d band of $[\text{Cu}(\text{anti-27})]^{2+}$ complex which did not shift after 1 sec. (1 sec = time required for mixing of anti-27 ligand and Cu^{2+} solution after addition).

$[\text{anti-27}] = [\text{Cu}^{2+}] = 5 \text{ mM}, T = 298 \text{ K}.$

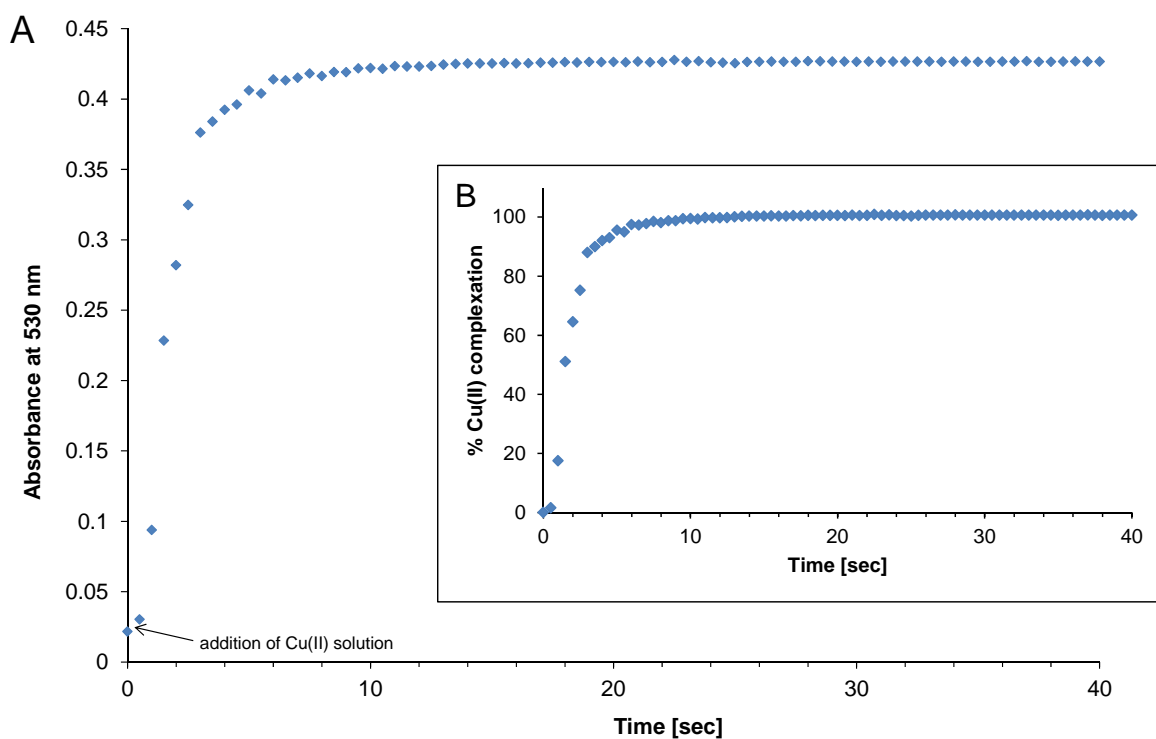


Figure S11. Time course of the copper(II) complexation by anti-27 ligand in aqueous ammonium acetate buffer. A) Absorbance at 530 nm of $[\text{Cu}(\text{anti-27})]^{2+}$ complex. B) % Cu(II) complexation.

$[\text{anti-27}] = [\text{Cu}^{2+}] = 5 \text{ mM}, T = 298 \text{ K}, \text{pH} = 6.5.$

Table S2. Values of Absorbance at 530 nm of $[\text{Cu}(\text{anti-27})]^{2+}$ complex and % Cu(II) complexation during the time course of the copper(II) complexation by *anti*-**27** ligand in aqueous ammonium acetate buffer. $[\text{anti-27}] = [\text{Cu}^{2+}] = 5 \text{ mM}$, $T = 298 \text{ K}$, pH = 6.5.

Time [sec]	Abs at 530 nm	% Cu(II) complexation
0	0.02168	0
0.5	0.030252	1.563
1	0.09382	17.455
1.5	0.228434	51.1085
2	0.281981	64.49525
2.5	0.324714	75.1785
3	0.376157	88.03925
3.5	0.383986	89.9965
4	0.392303	92.07575
4.5	0.396097	93.02425
5	0.406159	95.53975
5.5	0.40391	94.9775
6	0.413938	97.4845
6.5	0.413187	97.29675
7	0.415155	97.78875
7.5	0.418171	98.54275
8	0.416357	98.08925
8.5	0.419172	98.793
9	0.419086	98.7715
9.5	0.42179	99.4475
10	0.421995	99.49875
10.5	0.421525	99.38125
11	0.423388	99.847
11.5	0.423139	99.78475
12	0.423166	99.7915
12.5	0.423468	99.867
13	0.424483	100.12075
13.5	0.425038	100.2595
14	0.425326	100.3315
14.5	0.425223	100.30575
15	0.425209	100.30225
15.5	0.425527	100.38175
16	0.425287	100.32175
16.5	0.425405	100.35125
17	0.425859	100.46475
17.5	0.425782	100.4455
18	0.426266	100.5665
18.5	0.425963	100.49075
19	0.426387	100.59675
19.5	0.426205	100.55125
20	0.426386	100.5965

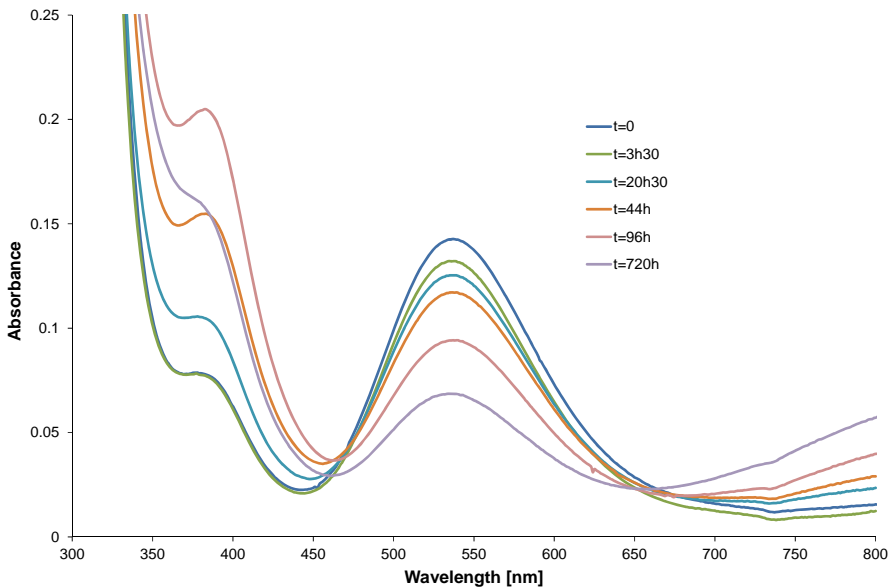


Figure S12. Visible absorption spectra of the complex $[\text{Cu}(\text{anti-27})]^{2+}$ in 5 M HCl solution at 50°C over time at 0, 3.5, 20.5, 44, 96 and 720 hours. [complex] = 2.35 mM

The behavior of the two bands at 370 and 530 nm over time are the same until $t = 96$ h. At the end of the measurements ($t = 720$ h) a slight modification of the band at 370 nm could be attributed to the degradation of the free ligand in these harsh conditions. No other complex seems to be formed, the λ_{max} of d-d band of $[\text{Cu}(\text{anti-27})]^{2+}$ complex did not change over the time.

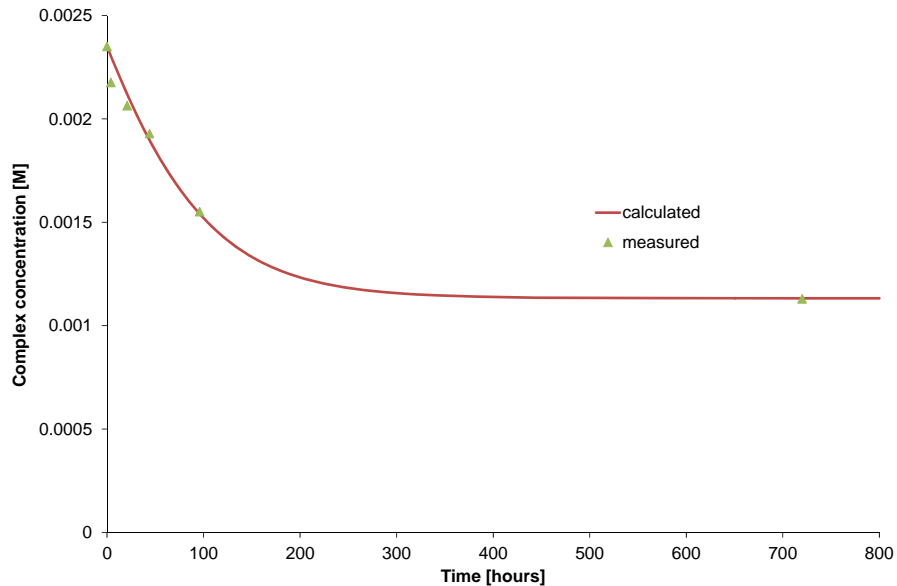


Figure S13. Fitting of experimental data at 530 nm with exponential curve of pseudo first order kinetics by the program Berkeley Madonna 8.3.18.

Characterization of compounds **1b-6b**

Cbz-(D)-ser(OTBDMS)-H **1b**

Prepared following the procedure described for compound **1a** with Z-(D)-ser(OTBDMS)-OMe. Yield: 69%, colorless oil. $[\alpha]_D^{20} -6.2$ (*c* 1.05, CHCl₃); ¹H NMR (250 MHz, CDCl₃): δ = 0.04 (s, 6H, H3'), 0.86 (s, 9H, H4'), 3.88 (dd, 1H, *J*_{gem} = 10.4 Hz, *J*_{4,5} = 4.1 Hz, H2'), 4.20 (dd, 1H, *J*_{gem} = 10.4 Hz, *J*_{4,5} = 2.7 Hz, H2'), 4.30-4.35 (m, 1H, H3), 5.14 (s, 2H, OCH₂Ph), 5.68 (d, 1H, *J*_{3,4} = 6.5 Hz, H2), 7.29-7.42 (m, 5H, H-Ar), 9.64 (s, 1H, H aldehyde); ¹³C NMR (62.9 MHz, CDCl₃): δ = -5.7 (2×C3'), 18.1 (OSiC(CH₃)₃), 25.7 (C4'), 61.1 (C3), 61.8 (C2'), 67.0 (OCH₂Ph), 128.0, 128.1, 128.4 (CH-Ar), 136.1 (C-Ar), 156.0 (C1), 198.7 (C4); IR: 3444, 3341, 2954, 2930, 2884, 2857, 1723, 1714, 1513.

Cbz-(D)-ser(OTBDMS)Ψ[CH₂NH] β Ala-OMe **2b**

Prepared following the procedure described for compound **2a** starting from **1b**. Yield: 61%, colorless oil. $[\alpha]_D^{20} -3.1$ (*c* 0.37, CHCl₃); ¹H NMR (250 MHz, CDCl₃): δ = 0.04 (s, 6H, H3'), 0.88 (s, 9H, H4'), 2.12 (s, 1H, NH), 2.50 (t, 2H, *J* = 6.3Hz, H6), 2.66 (dd, 1H, *J*_{gem} = 12.0Hz, *J*_{3,4} = 5.5Hz, H4), 2.80-2.94 (m, 3H, H4, H5), 3.59-3.80 (m, 6H, H2', H3, H8), 5.11 (s, 2H, OCH₂Ph), 5.31 (s, 1H, H2), 7.23-7.36 (m, 5H, H-Ar); ¹³C NMR (62.9 MHz, CDCl₃): δ = -5.6 (2×C3'), 18.1 (OSiC(CH₃)₃), 25.8 (C4'), 34.6 (C6), 45.0 (C5), 50.0 (C4), 51.5 (C3), 51.6 (C8), 63.3 (C2'), 66.7 (OCH₂Ph), 128.1, 128.5 (CH-Ar), 136.5 (C-Ar), 156.2 (C1), 173.0 (C7); IR: 3337, 2953, 2929, 2884, 2856, 2333, 2170, 1720, 1527; MS (HR-ESI) calcd for C₂₁H₃₆N₂O₅Si [M+H]⁺ 425.2466, found: 425.2478.

Cbz-(D)-ser(OTBDMS)Ψ[CH₂NBoc] β Ala-OMe **3b**

Prepared following the procedure described for compound **3a** starting from **2b**. Yield 98%, colorless oil; $[\alpha]_D^{20} -6.9$ (*c* 1.32, CHCl₃); ¹H NMR (250 MHz, CDCl₃): δ = -0.07 (s, 6H, H3'), 0.91 (s, 9H, H4'), 1.46 (s, 9H, (CH₃)₃), 2.59 (br s, 2H, H6), 3.15-3.24 (m, 1H, H4), 3.34-3.69 (m, 8H, H4, H5, H8, H2'), 3.90 (br s, 1H, H3), 5.11 (br s, 2.5H, H2, OCH₂Ph), 5.61 (br s, 0.5H, H2), 7.35 (s, 5H, H-Ar); ¹³C NMR (62.9 MHz, CDCl₃): δ = -5.6 (2xC3'), 18.2 (OSiC(CH₃)₃), 25.8 (C4'), 28.3 (C(CH₃)₃), 33.0, 33.6 (C6), 44.0 (C5), 48.4 (C4), 51.6 (C8), 52.5 (C3), 63.2 (C2'), 66.4 (OCH₂Ph), 80.3 (C(CH₃)₃), 127.9, 128.4 (CH-Ar), 136.6 (C-Ar), 155.2, 155.9, 156.3, 156.6 (C1, CO), 172.0,

172.4 (C7); IR: 3450, 3346, 2953, 2928, 2857, 1733, 1727, 1698, 1510; MS (HR-ESI) calcd for $C_{26}H_{44}N_2NaO_7 [M+Na]^+$ 547.2816, found: 547.2816

Cbz-(D)-ser(OH) Ψ [CH₂NBoc] β Ala-OMe **4b**

Prepared following the procedure described for compound **4a** starting from **3b**. Yield: 81%, colorless oil. $[\alpha]_D^{20} = -3.0$ (*c* 0.80, CHCl₃); ¹H NMR (250 MHz, CDCl₃): $\delta = 1.45$ (s, 9H, (CH₃)₃), , 2.58 (t, 2H, $J_{5,6} = 7.0$ Hz, H6), 3.13 (dd, 1H, $J_{\text{gem}} = 13.7$ Hz, $J_{3,4} = 4.3$ Hz, H4), 3.40-3.84 (m, 10H, H3, H4, H5, H8, H2', H3'), 5.09 (s, 2H, OCH₂Ph), 5.45 (d, 1H, $J_{2,3} = 7.5$ Hz, H2), 7.34 (s, 5H, H-Ar); ¹³C NMR (62.9 MHz, CDCl₃): $\delta = 28.2$ (C(CH₃)₃), 33.5 (C6), 44.2 (C5), 46.7 (C4), 51.1 (C3), 51.7 (C8), 61.2 (C2'), 66.7 (OCH₂Ph), 81.3 (C(CH₃)₃), 128.0, 128.1, 128.5 (CH-Ar), 136.4 (C-Ar), 156.1 (C1), 157.1 (CO), 171.7 (C7); IR: 3421, 3357, 2974, 1723, 1697, 1526. MS (HR-ESI) calcd for $C_{20}H_{30}N_2NaO_7 [M+Na]^+$ 433.1945, found: 433.1949.

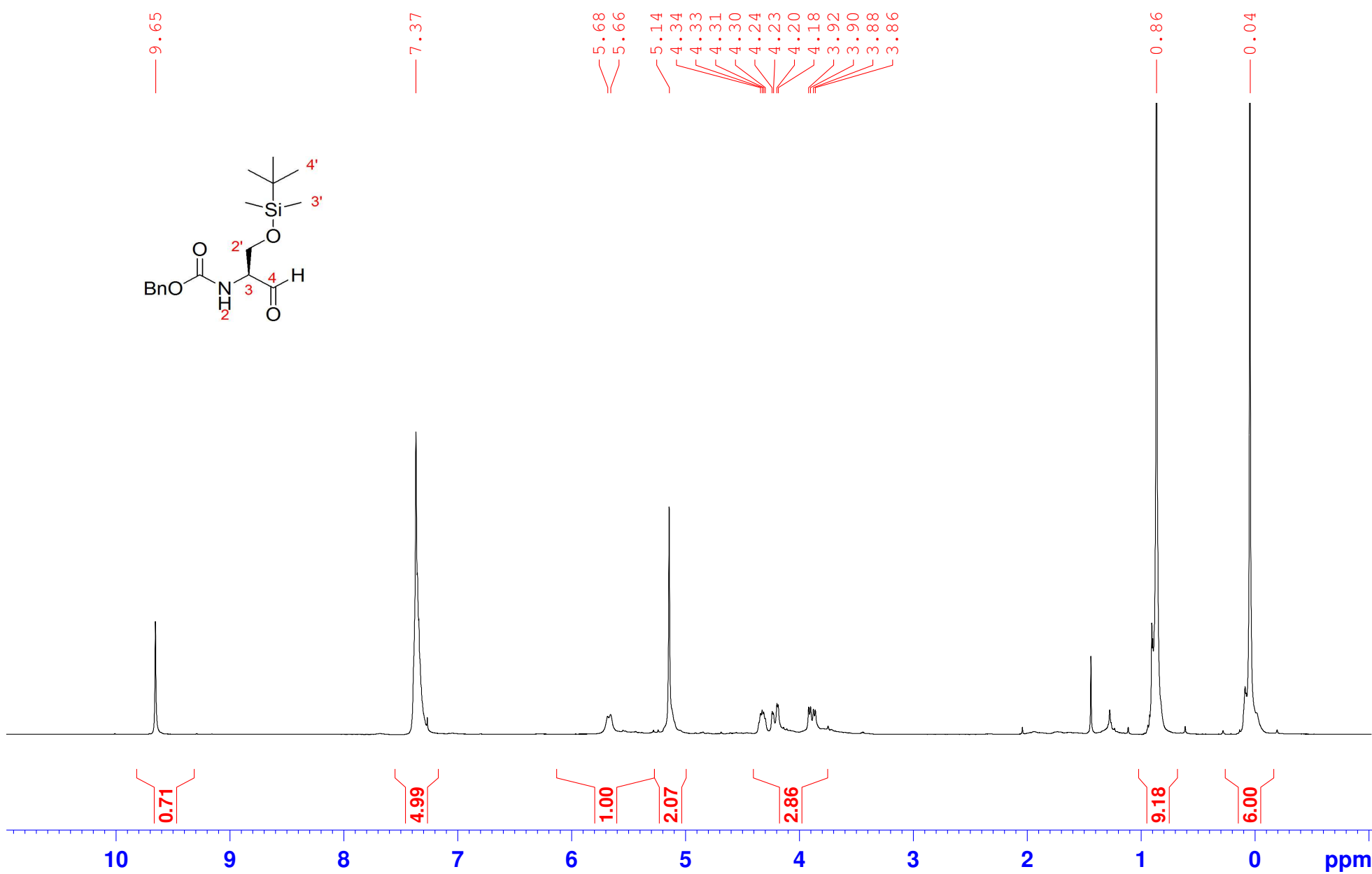
Cbz-(D)-Ser(OTs) Ψ [CH₂NBoc] β Ala-OMe **5b**

Prepared following the procedure described for compound **5a** starting from **4b**. Yield: 91%, colorless oil. $[\alpha]_D^{20} -1.9$ (*c* 0.82, CHCl₃); ¹H NMR (400 MHz, CDCl₃): $\delta = 1.44$ (s, 9H, (C(CH₃)₃), 2.46 (s, 3H, H4'), 2.55 (br s, 2H, H6), 3.16-3.65 (m, 4H, H4, H5), 3.69 (s, 3H, H8), 4.06 (br s, 3H, H2', H3), 5.00-5.16 (m, 2.5H, OCH₂Ph, H2), 5.69 (s, 0.5H, H2), 7.32 (m, 7H, H-Ar, H3'), 7.80 (d, 2H, $J = 8.2$ Hz, H3'); ¹³C NMR (100 MHz, CDCl₃): $\delta = 21.7$ (C4'), 28.2 (C(CH₃)₃), 33.0, 33.6 (C6), 44.3 (C5), 48.1 (C4), 49.6, 50.2 (C3), 51.8 (C8), 66.7, 66.9 (OCH₂Ph), 69.2 (C2'), 80.9 (C(CH₃)₃), 127.9 (C3'), 128.0, 128.4 (CH-Ar), 130.0 (C3'), 132.4 (C-Ar), 136.3 (C-Ar), 145.1 (C-Ar), 156.0 (C1), 156.6 (CO), 172.0 (C7); IR (film, ν , cm⁻¹): 3336, 2975, 2952, 1731, 1697, 1598, 1522, 1438, 1417, 1366, 1240; MS (HR-ESI) calcd for $C_{27}H_{36}N_2O_9SNa [M+Na]^+$ 587.2084, found: 587.2044.

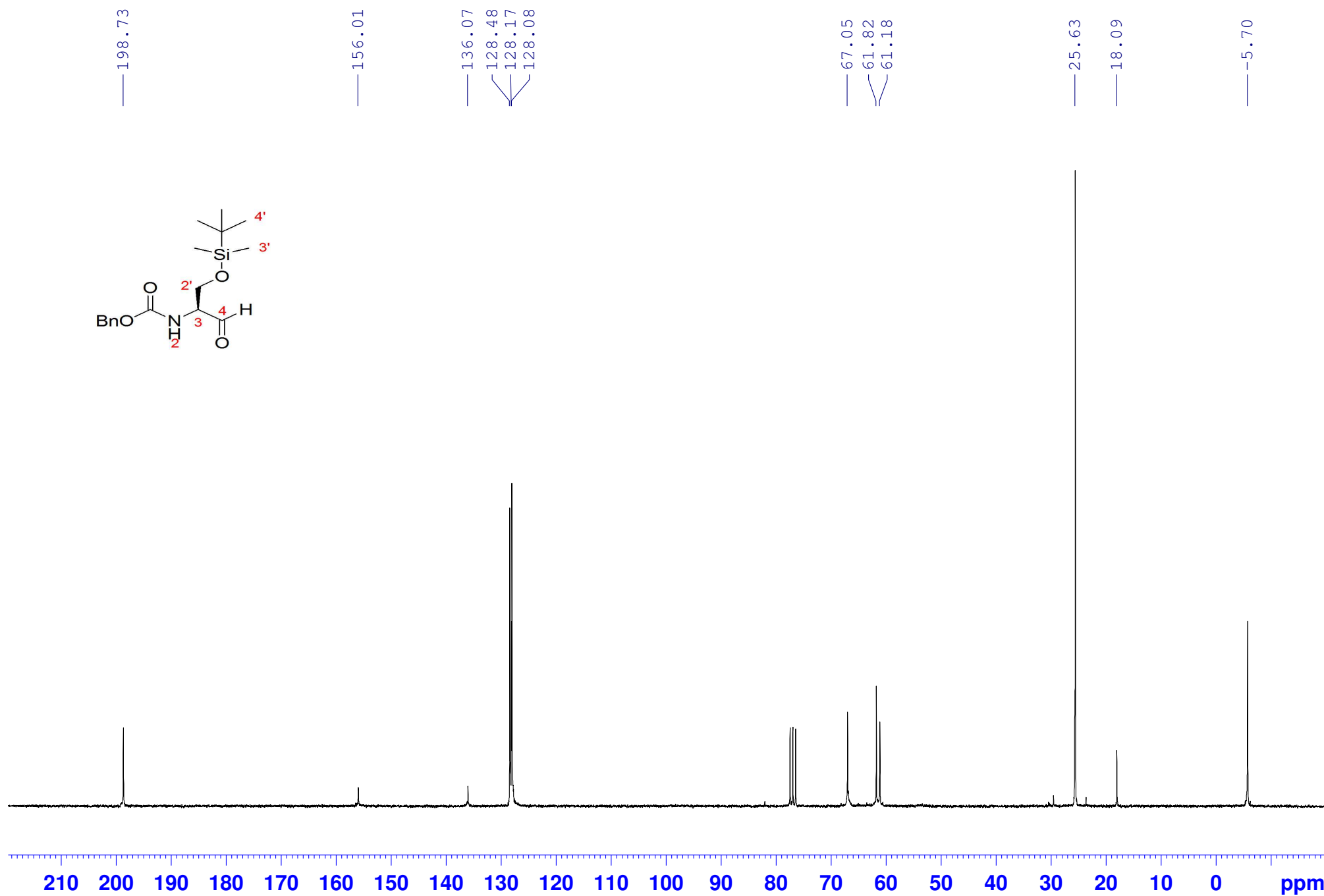
Compound **6b**

Prepared following the procedure described for compound **6a** starting from **5b**. Yield: 94%, colorless oil. $[\alpha]_D^{20} -0.5$ (*c* 0.43, CHCl₃); ¹H NMR (400 MHz, CDCl₃): $\delta = 1.45$ (s, 9H, (C(CH₃)₃), 2.57 (br s, 2H, H6), 3.16-3.62 (m, 6H, H4, H5, H2'), 3.69 (s, 3H, H8), 3.98 (br s, 1H, H3), 5.10-5.22 (m, 2.5H, OCH₂Ph, H2), 5.75 (br s, 0.5H, H2), 7.32-7.35 (m, 5H, H-Ar); ¹³C NMR (100 MHz, CDCl₃): $\delta = 28.2$ (C(CH₃)₃), 33.0, 33.6 (C6), 44.1 (C5), 48.5, 49.0 (C4), 50.1, 50.9 (C3), 51.7 (C8), 52.5 (C2'), 66.6 (OCH₂Ph), 80.8 (C(CH₃)₃), 127.9, 128.0, 128.4 (CH-Ar), 136.4 (C-Ar), 154.9 (CO), 155.8, 156.1 (C1), 156.6 (CO), 172.5, 172.5 (C7); IR: 3334, 2976, 2947, 2103, 1728, 1697, 1530; MS (HR-ESI) calcd for $C_{20}H_{29}N_5O_6Na [M+Na]^+$ 458.2010, found: 458.2023.

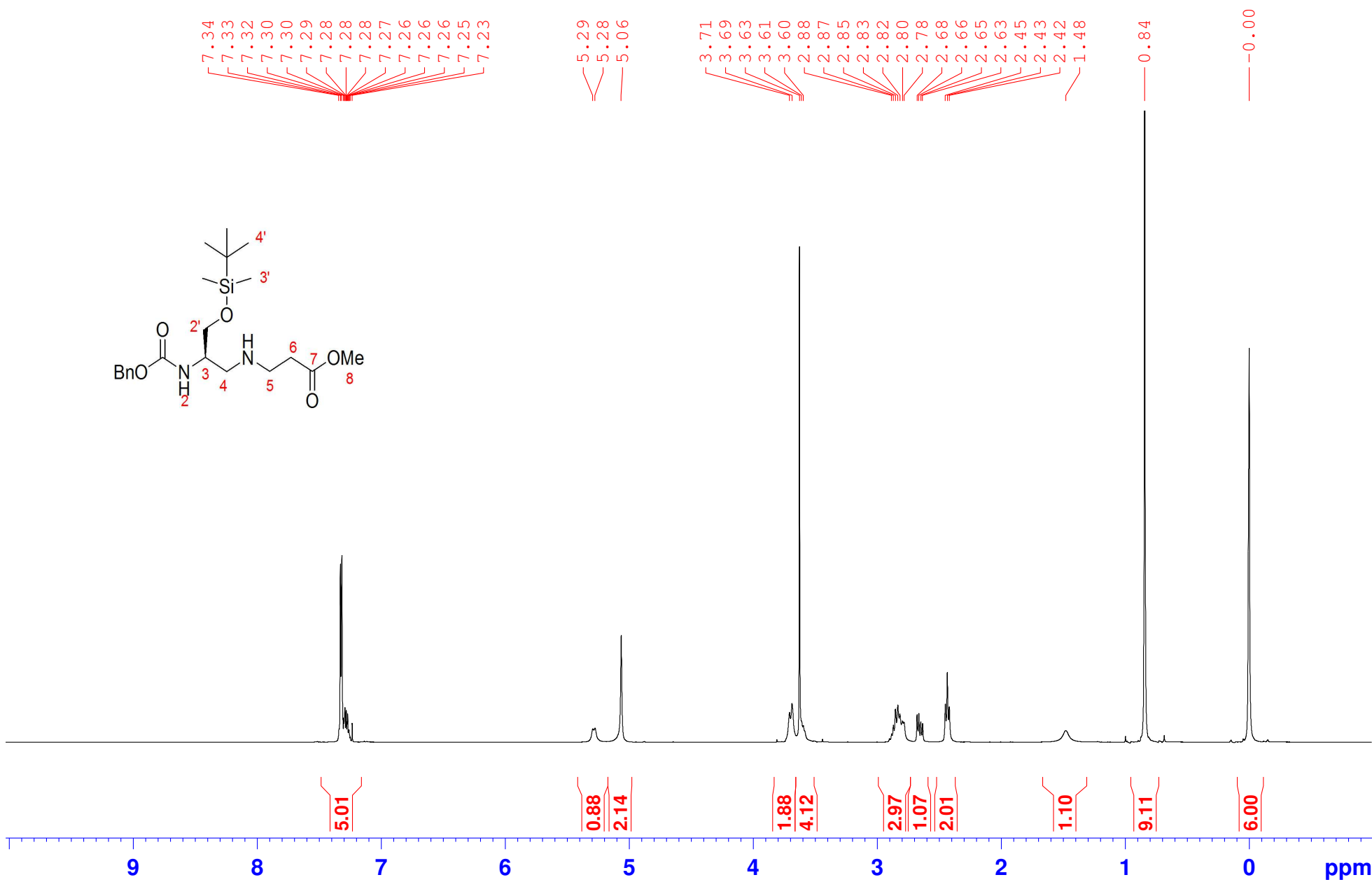
compound 1a, 250 MHz, CDCl₃



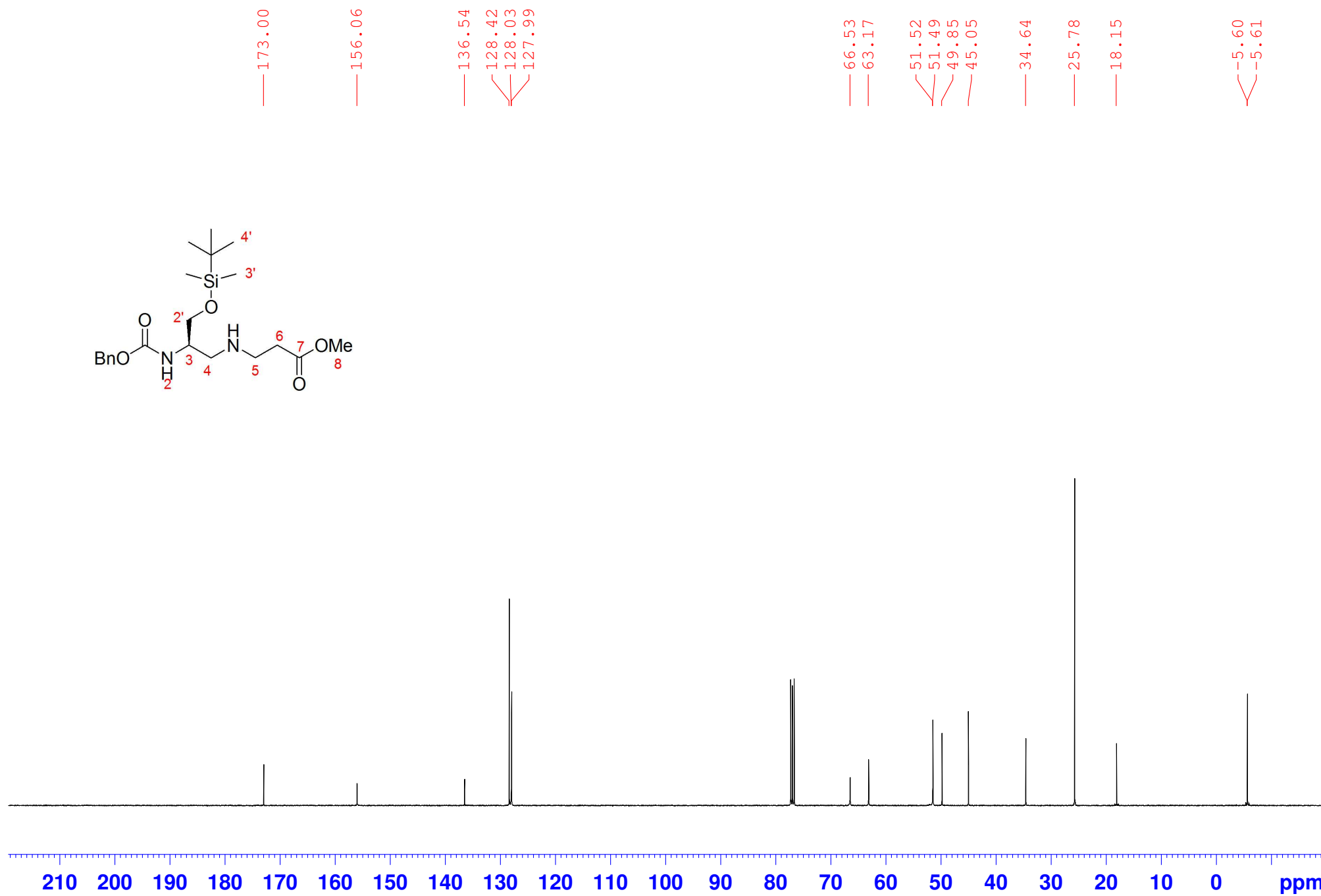
Compound 1a, 62.9 MHz, CDCl₃



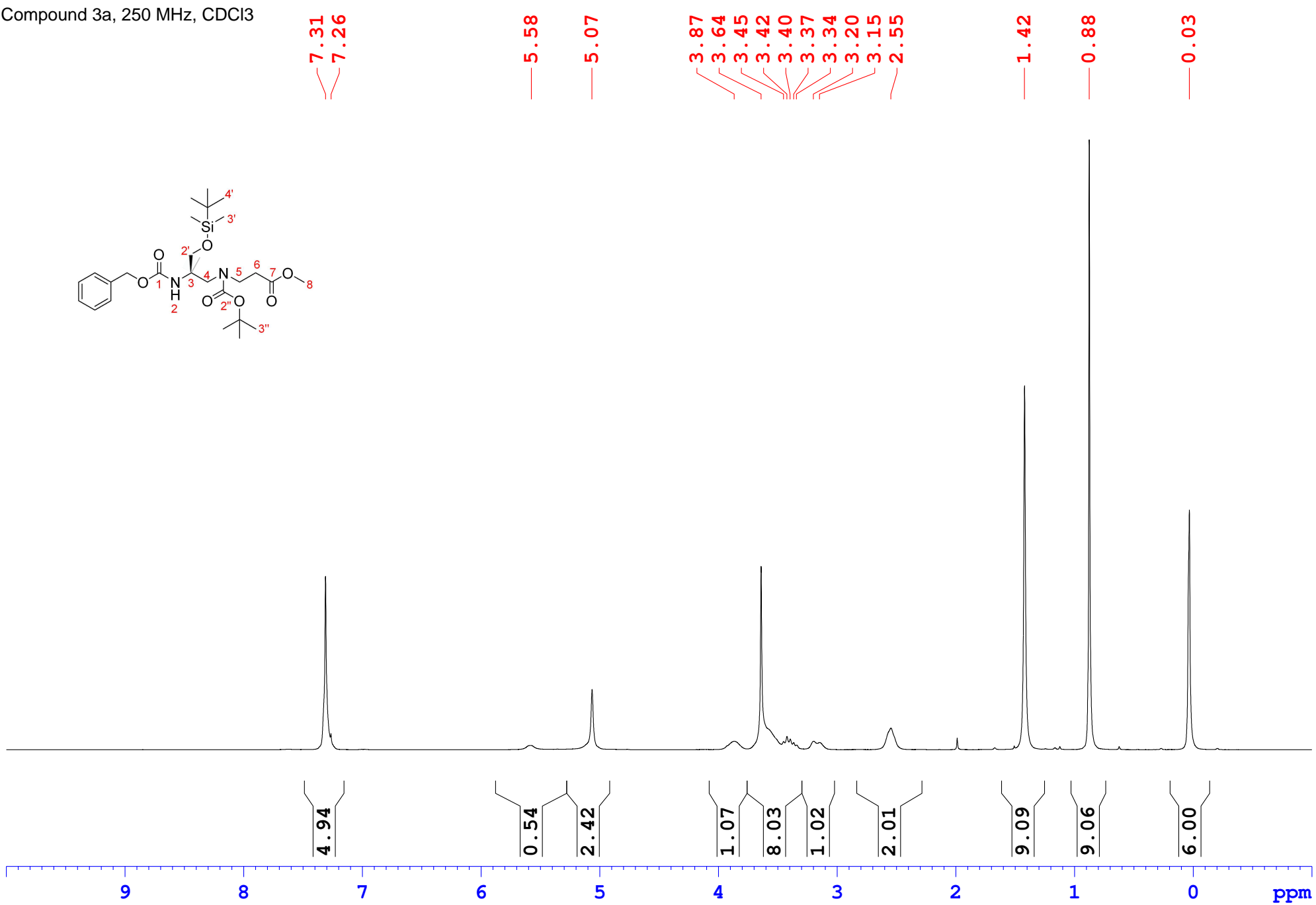
Compound 2a, 250 MHz, CDCl₃



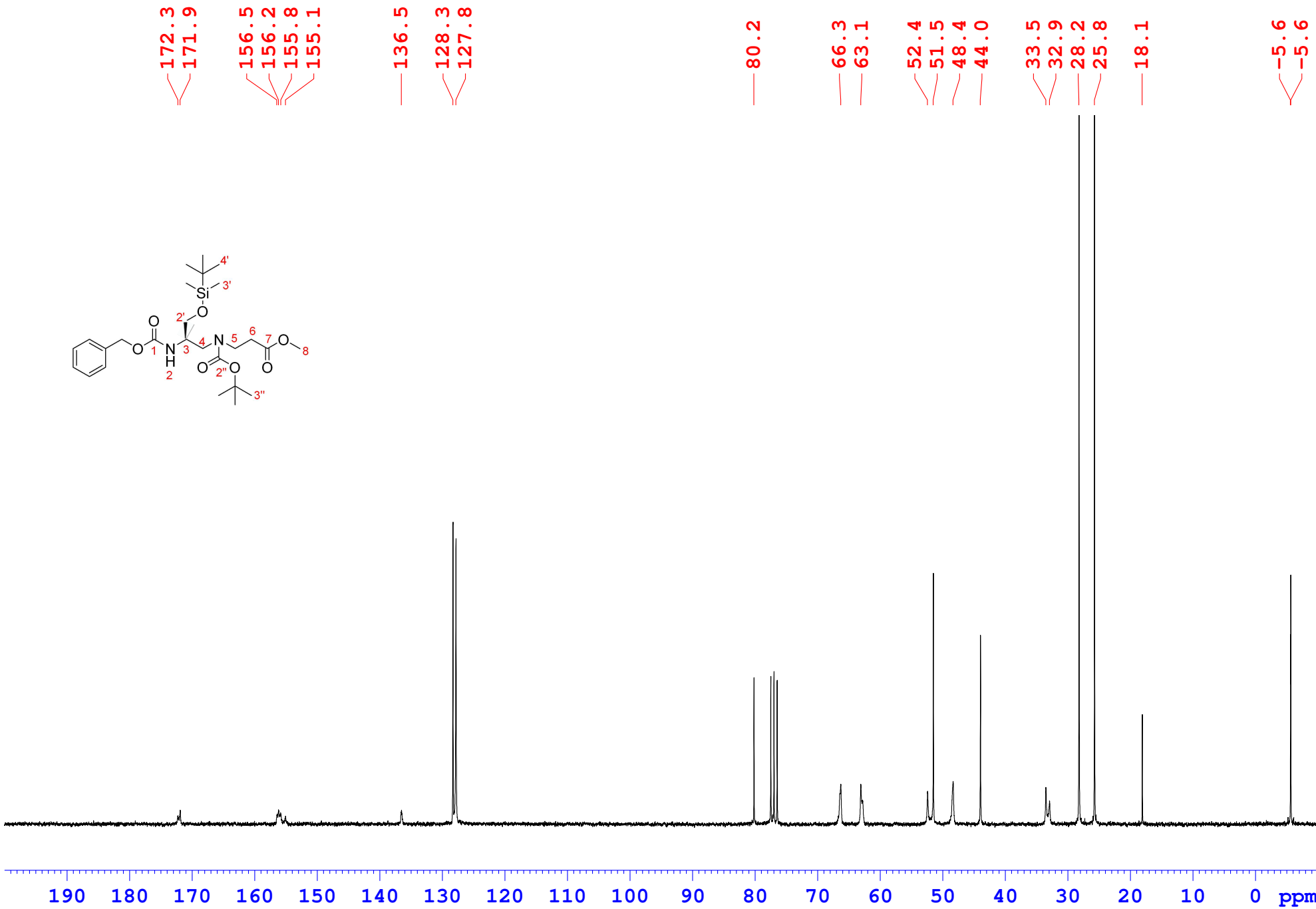
Compound 2a, 62.9 MHz, CDCl₃



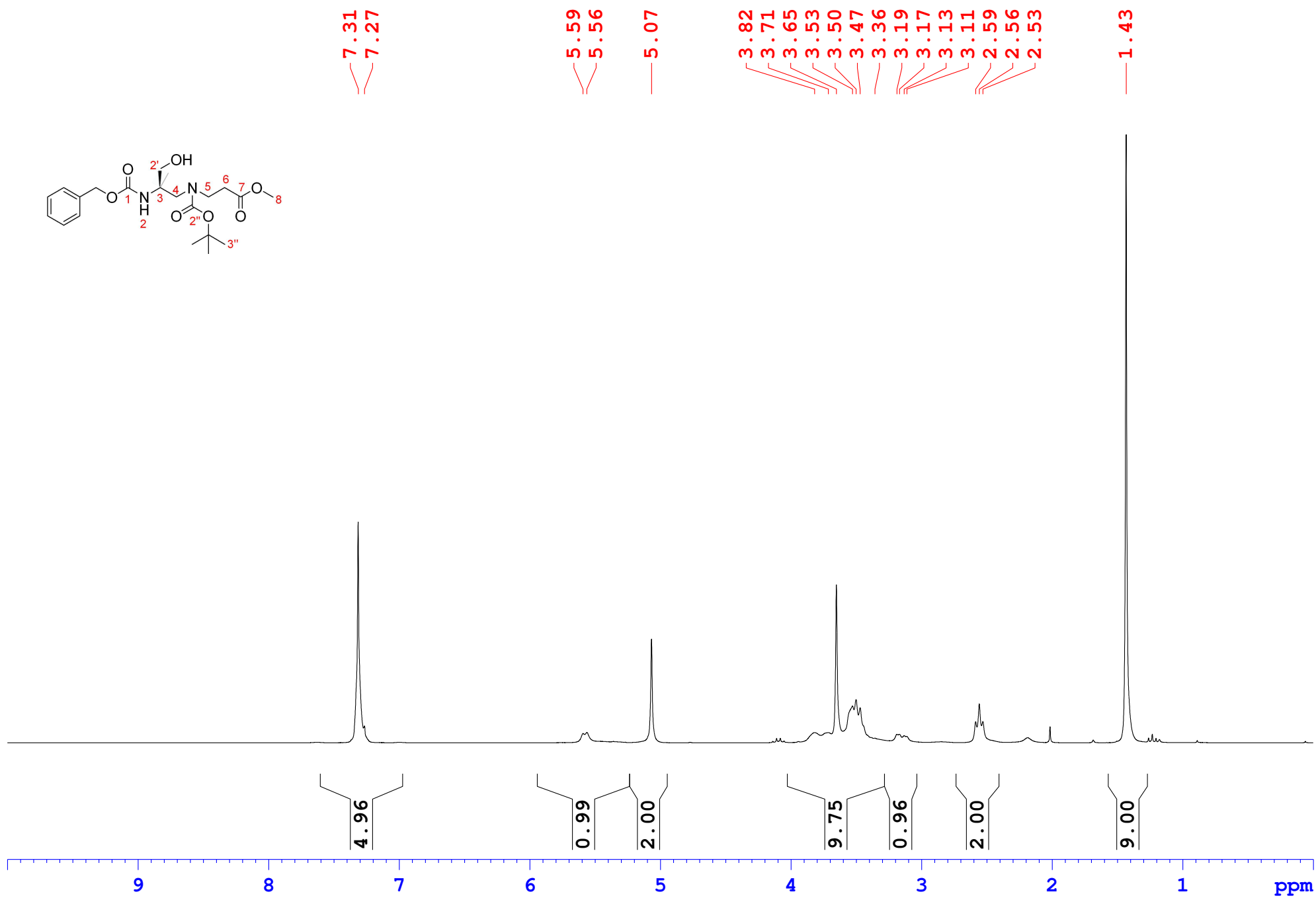
Compound 3a, 250 MHz, CDCl₃



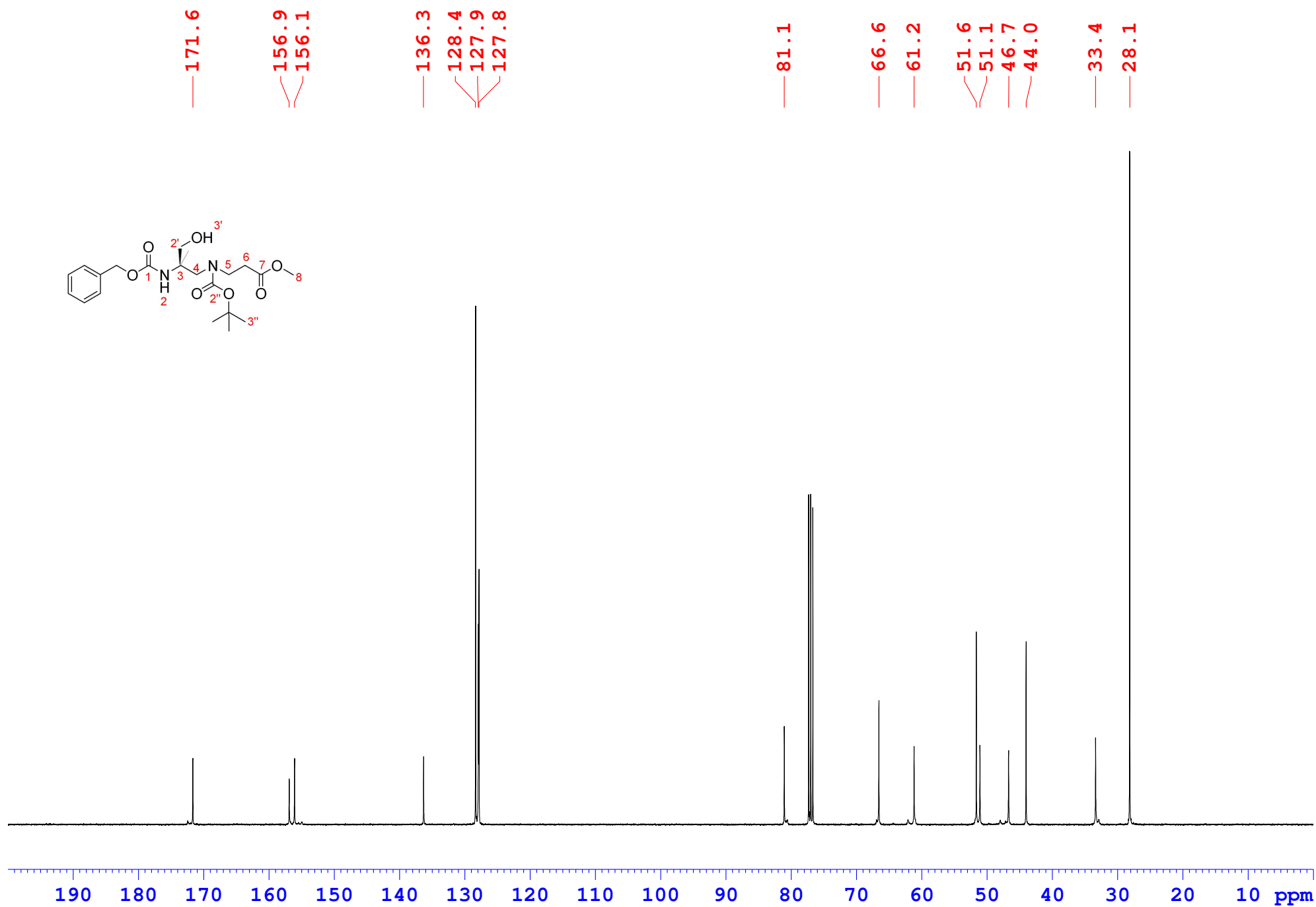
Compound 3a, 250 MHz, CDCl₃



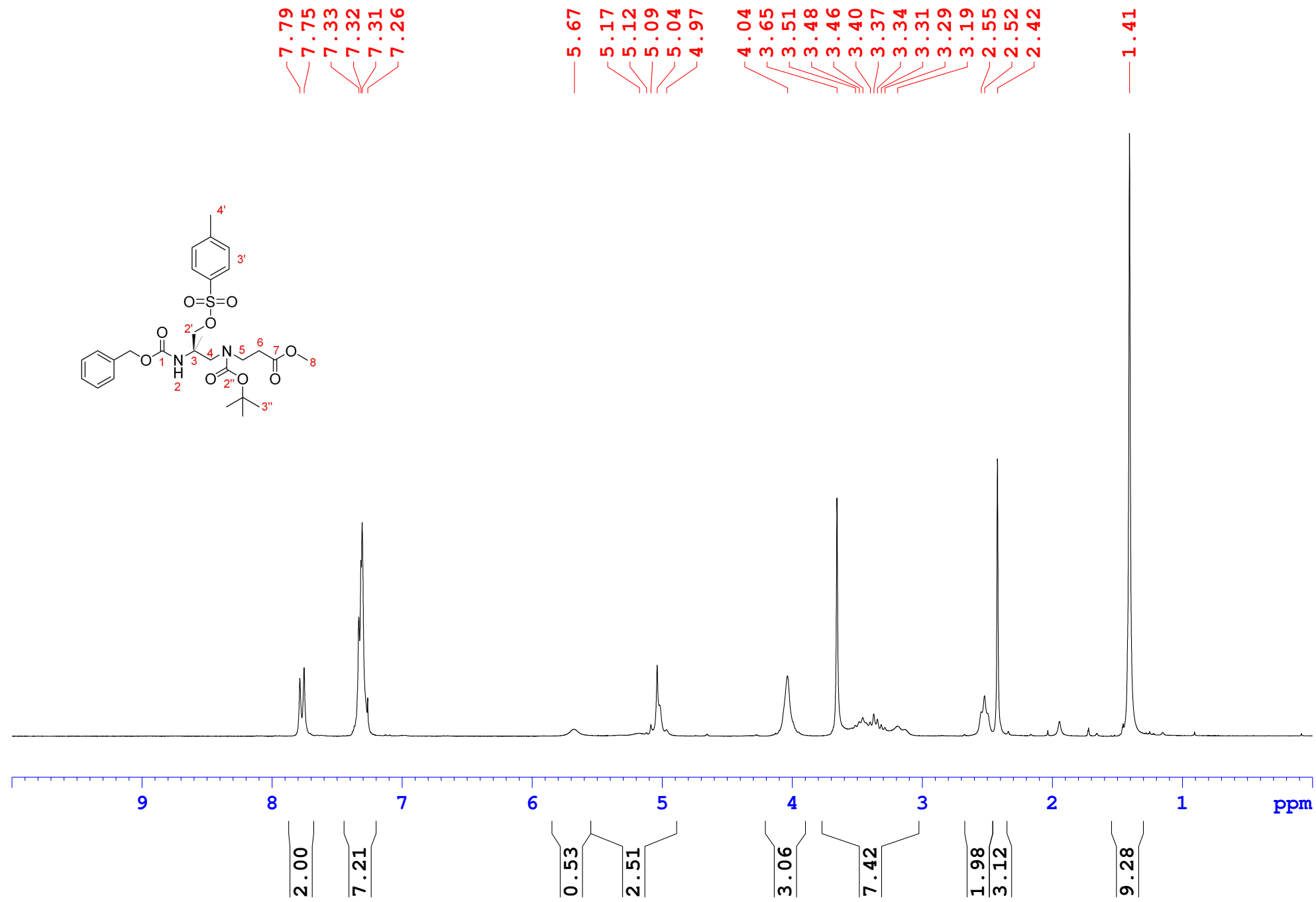
Compound 4a, 400 MHz, CDCl₃



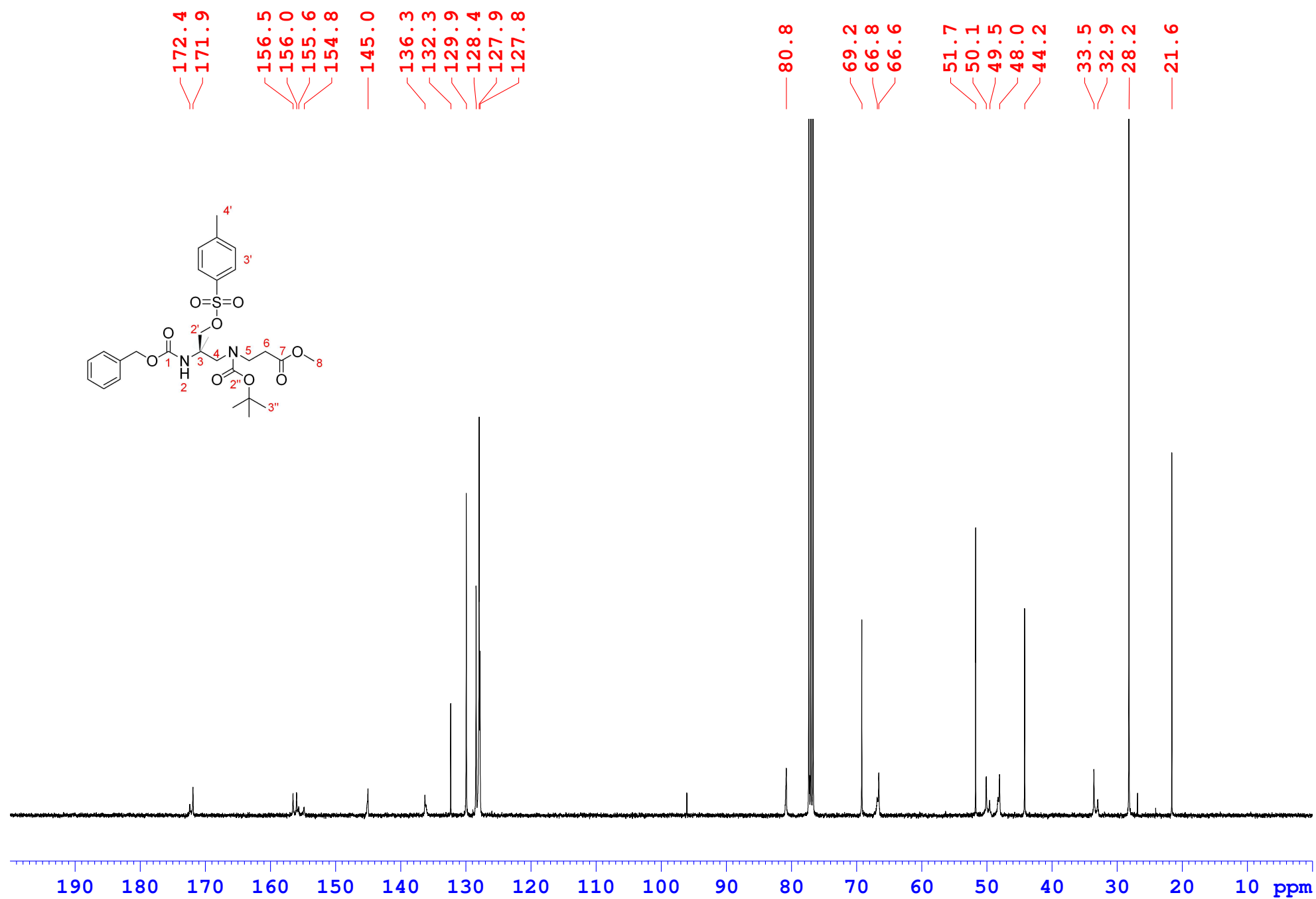
Compound 4a, 100 MHz, CDCl₃



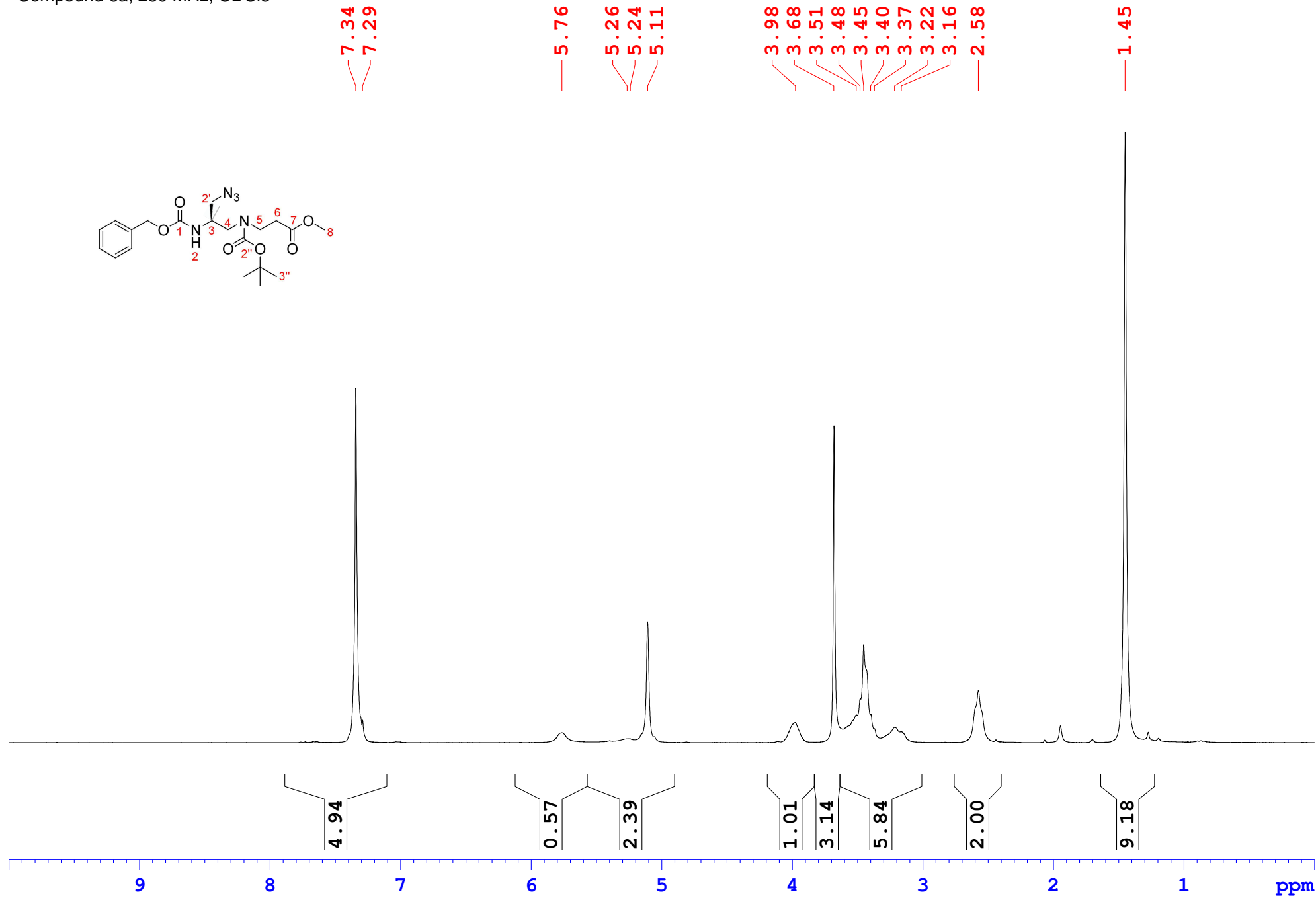
Compound 5a, 250 MHz, CDCl₃



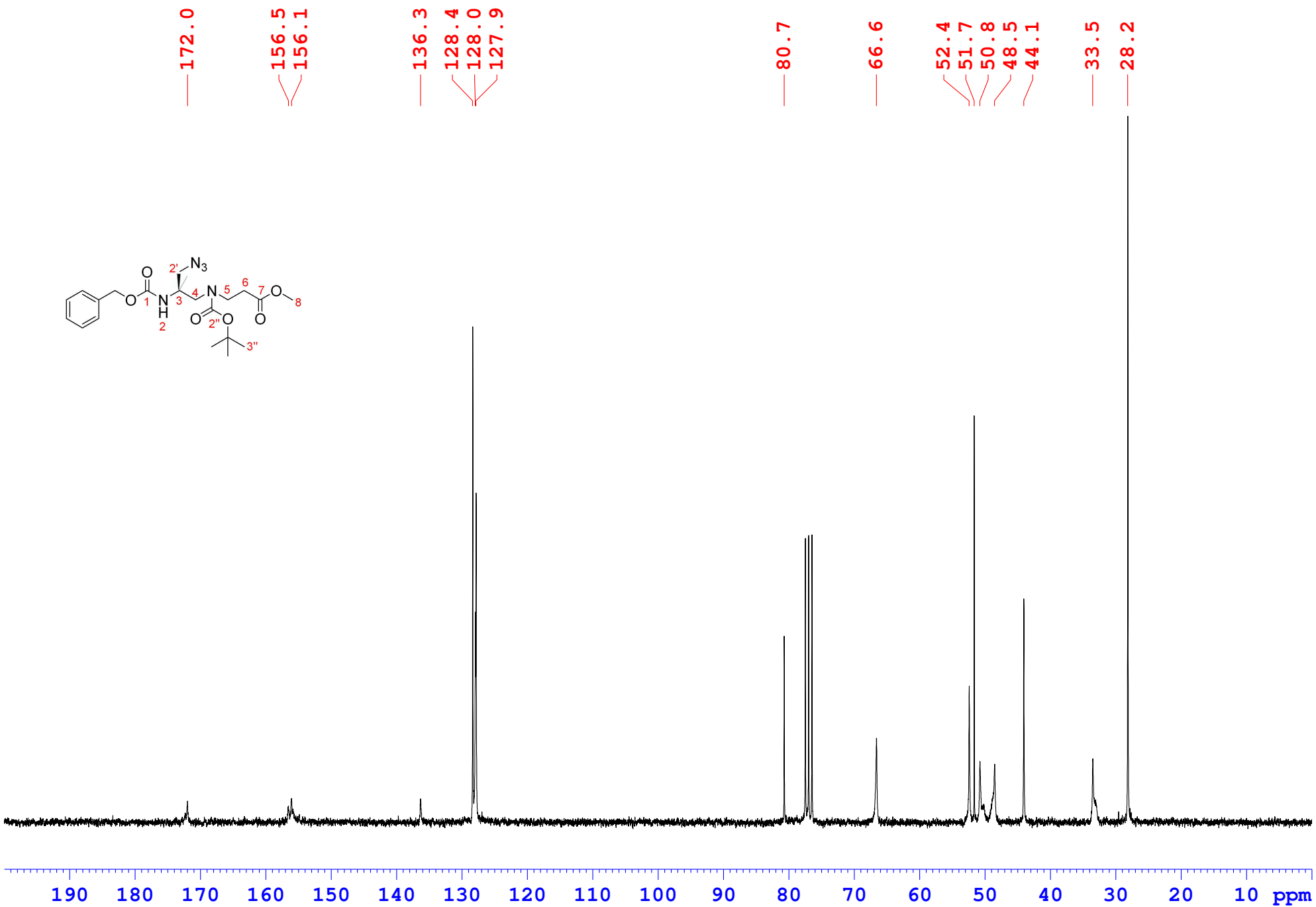
Compound 5a, 100 MHz, CDCl₃



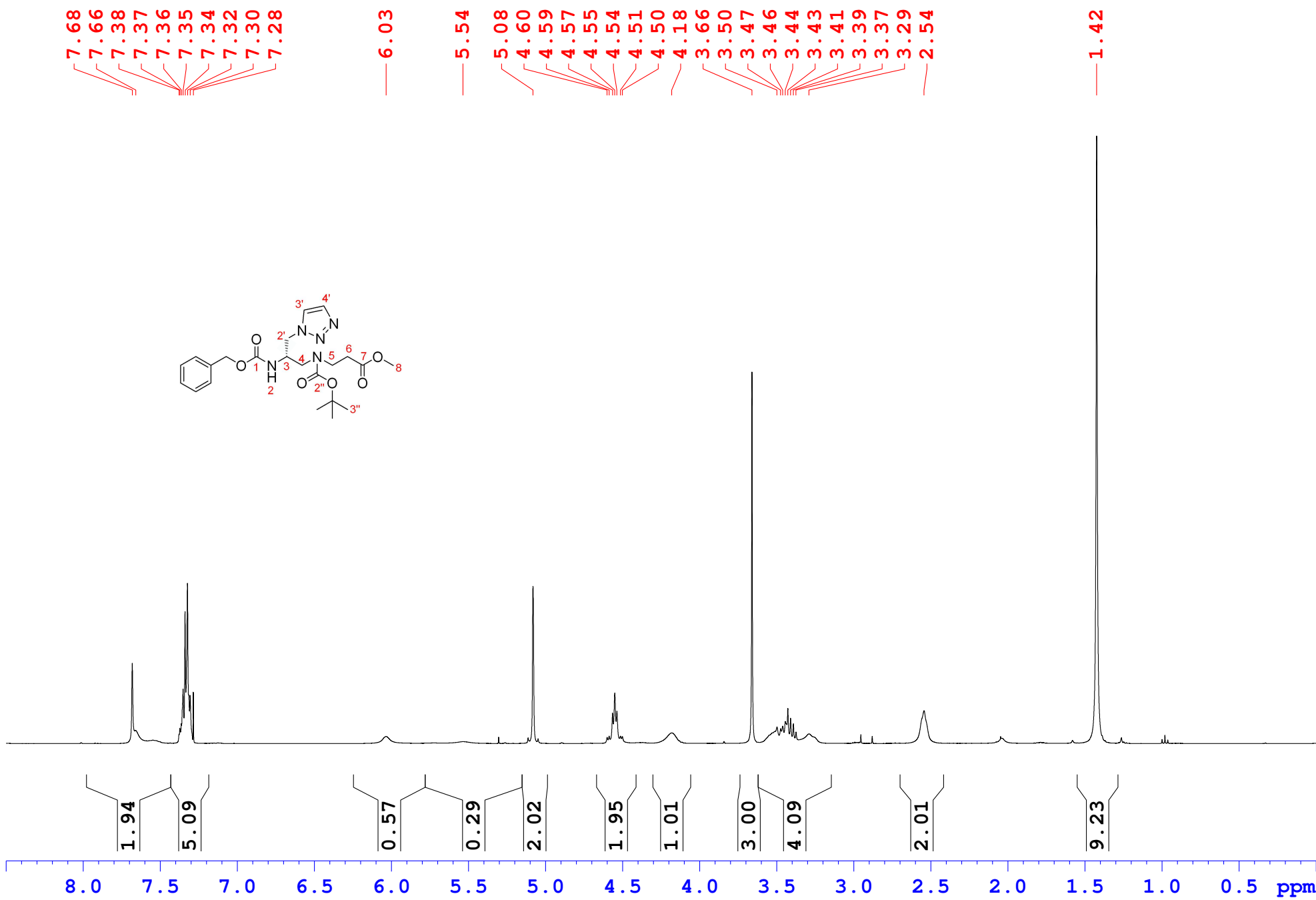
Compound 6a, 250 MHz, CDCl₃



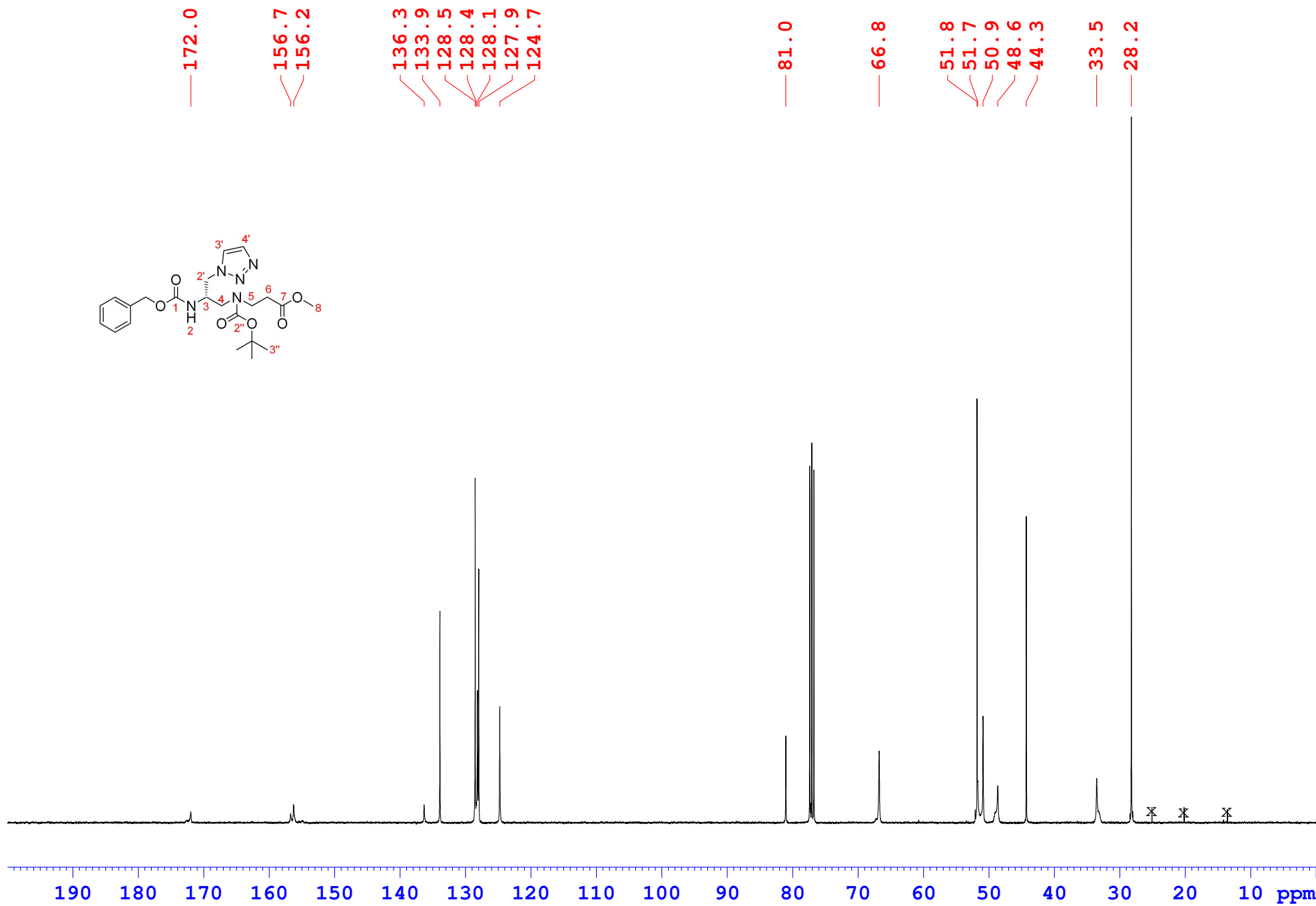
Compound 6a, 62.9MHz, CDCl₃



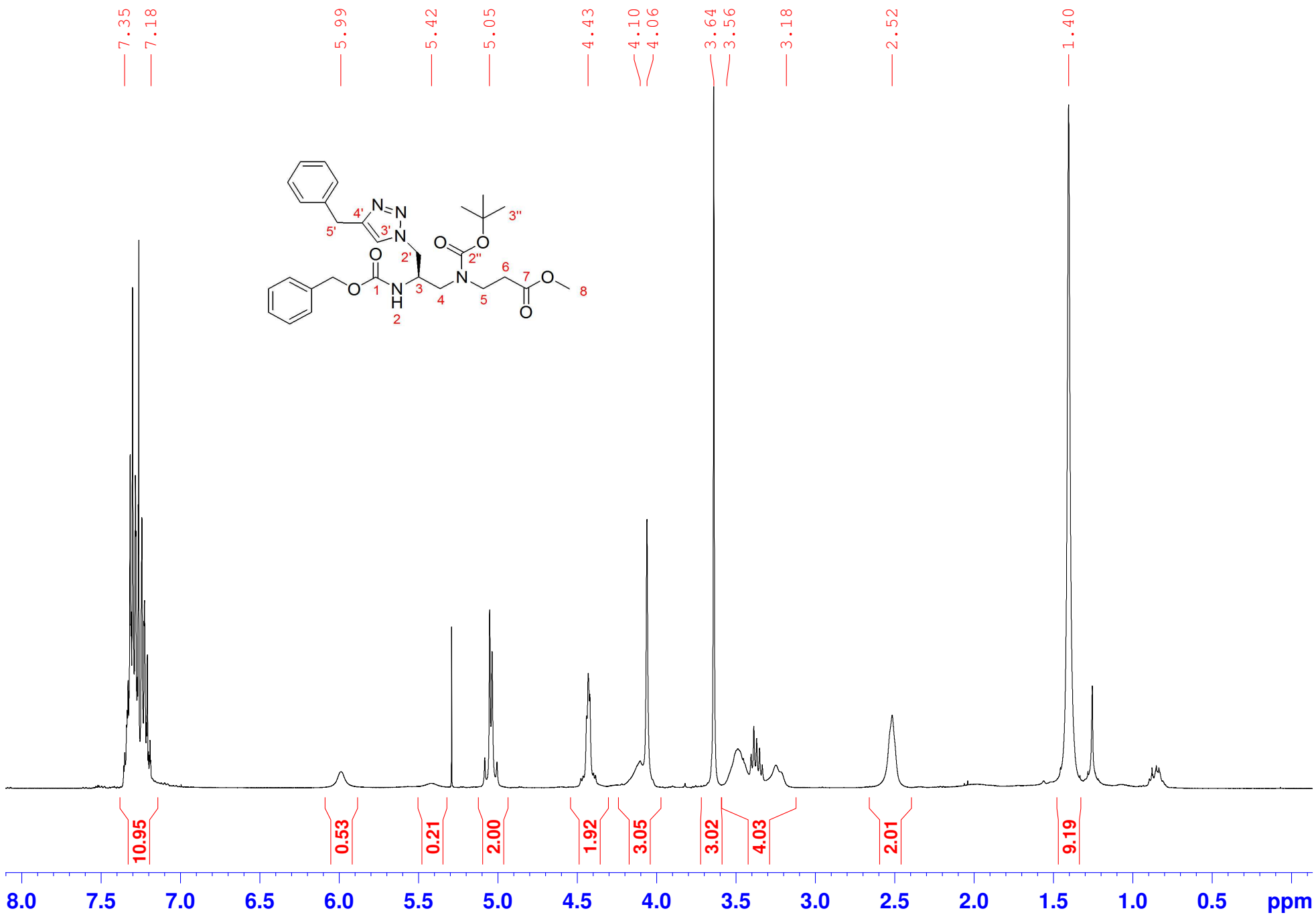
Compound 9, 400 MHz, CDCl₃



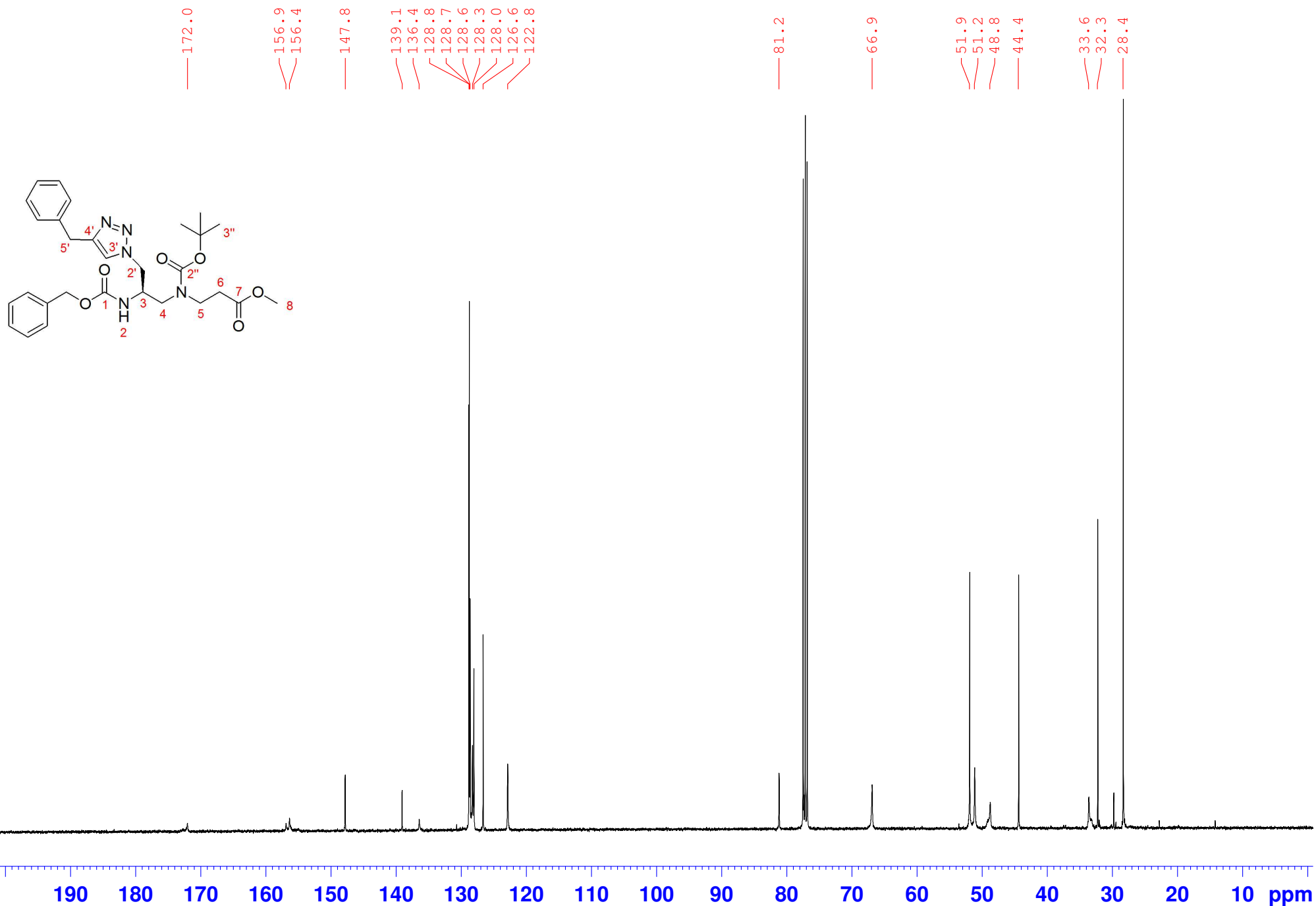
Compound 9, 100 MHz, CDCl₃



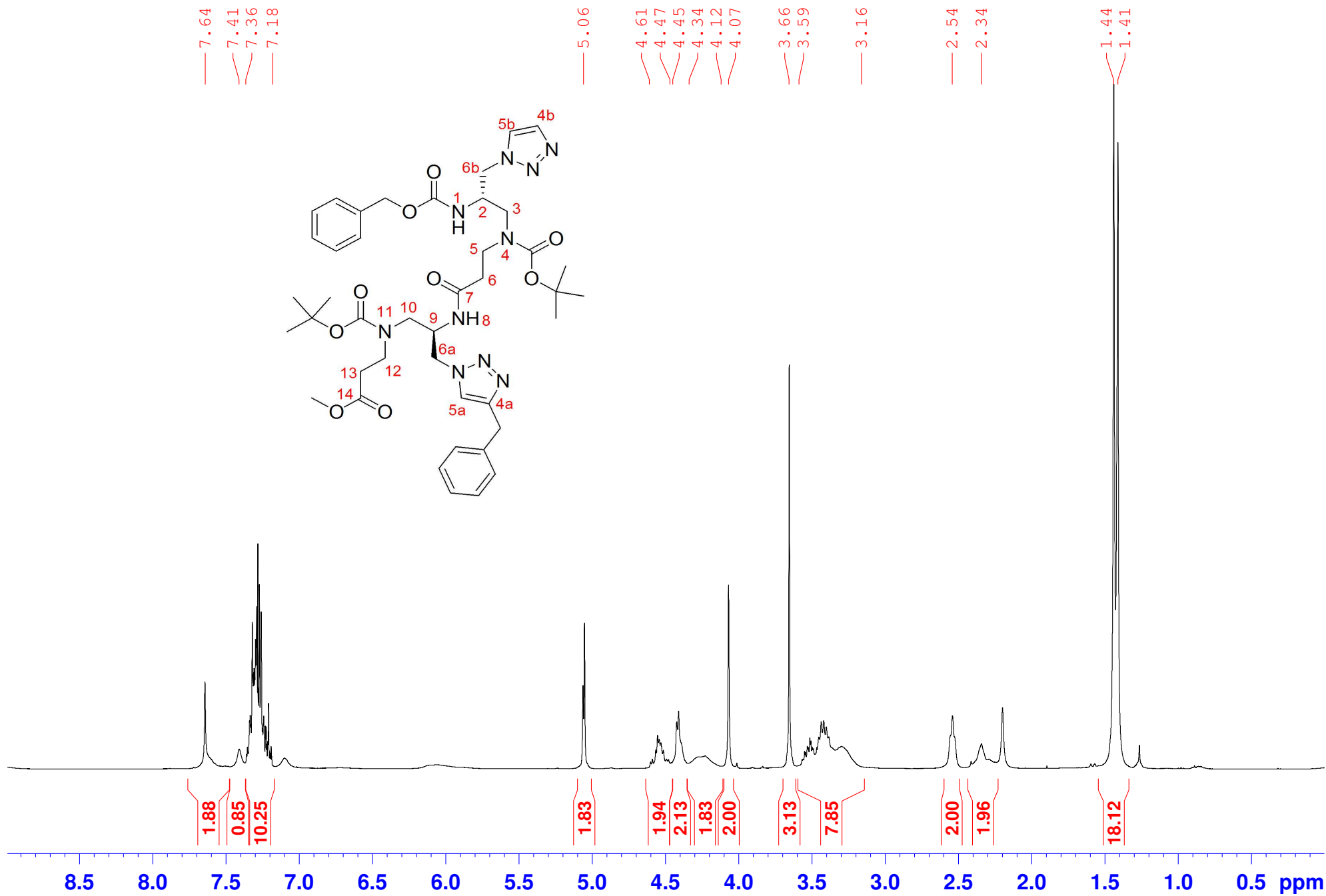
Compound 7, 400 MHz, CDCl₃



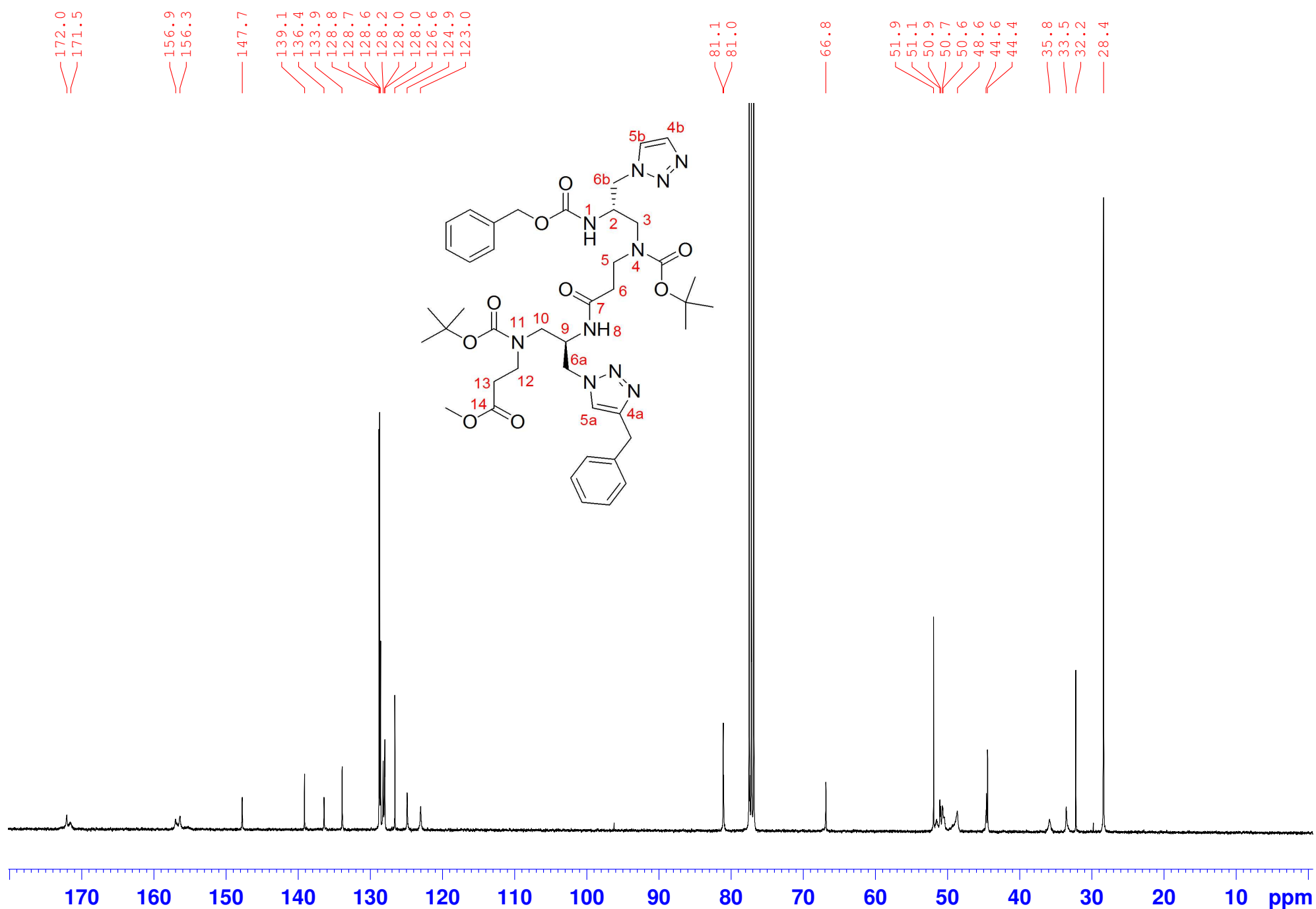
Compound 7, 100 MHz, CDCl₃



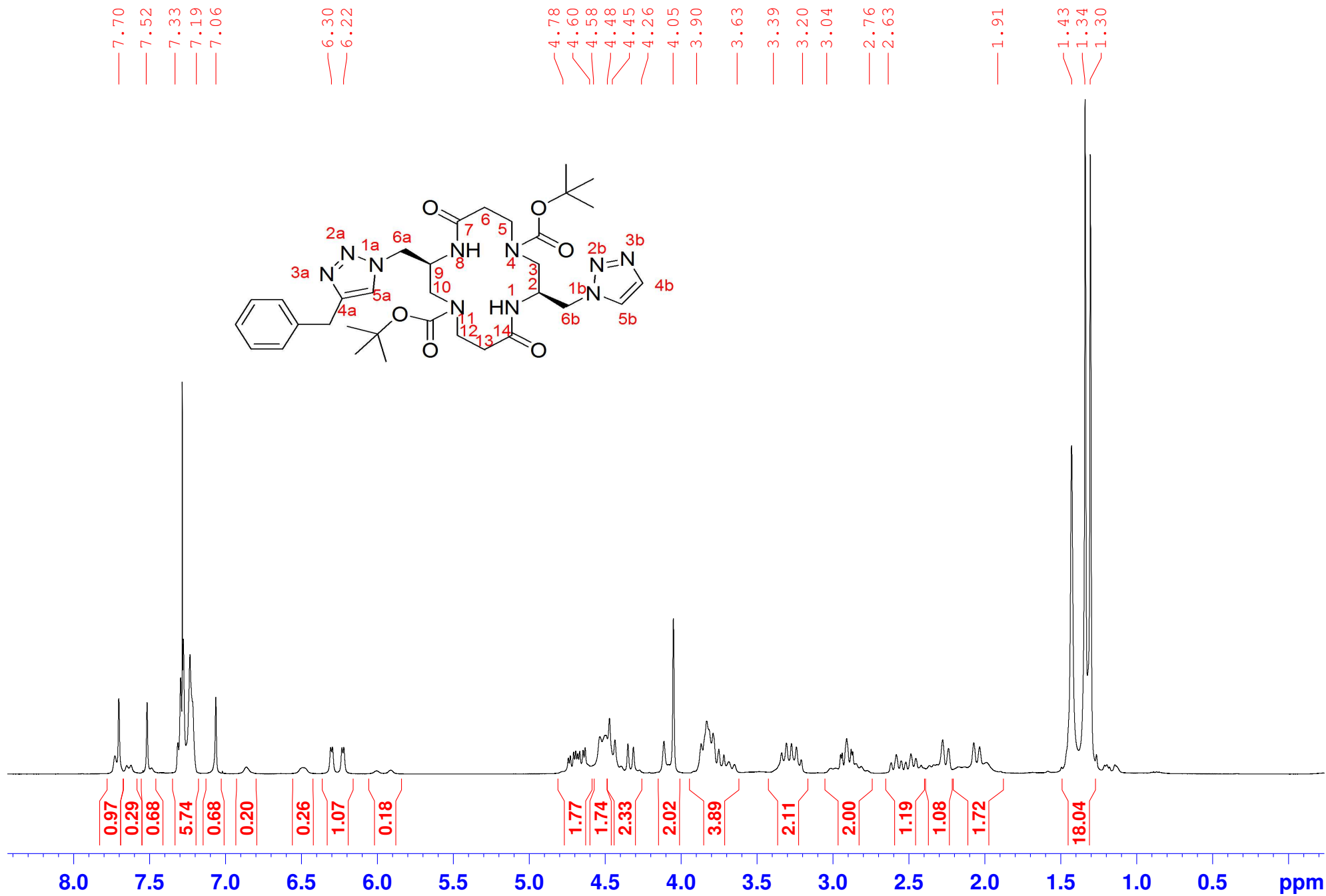
Compound 13, 400 MHz, CDCl₃



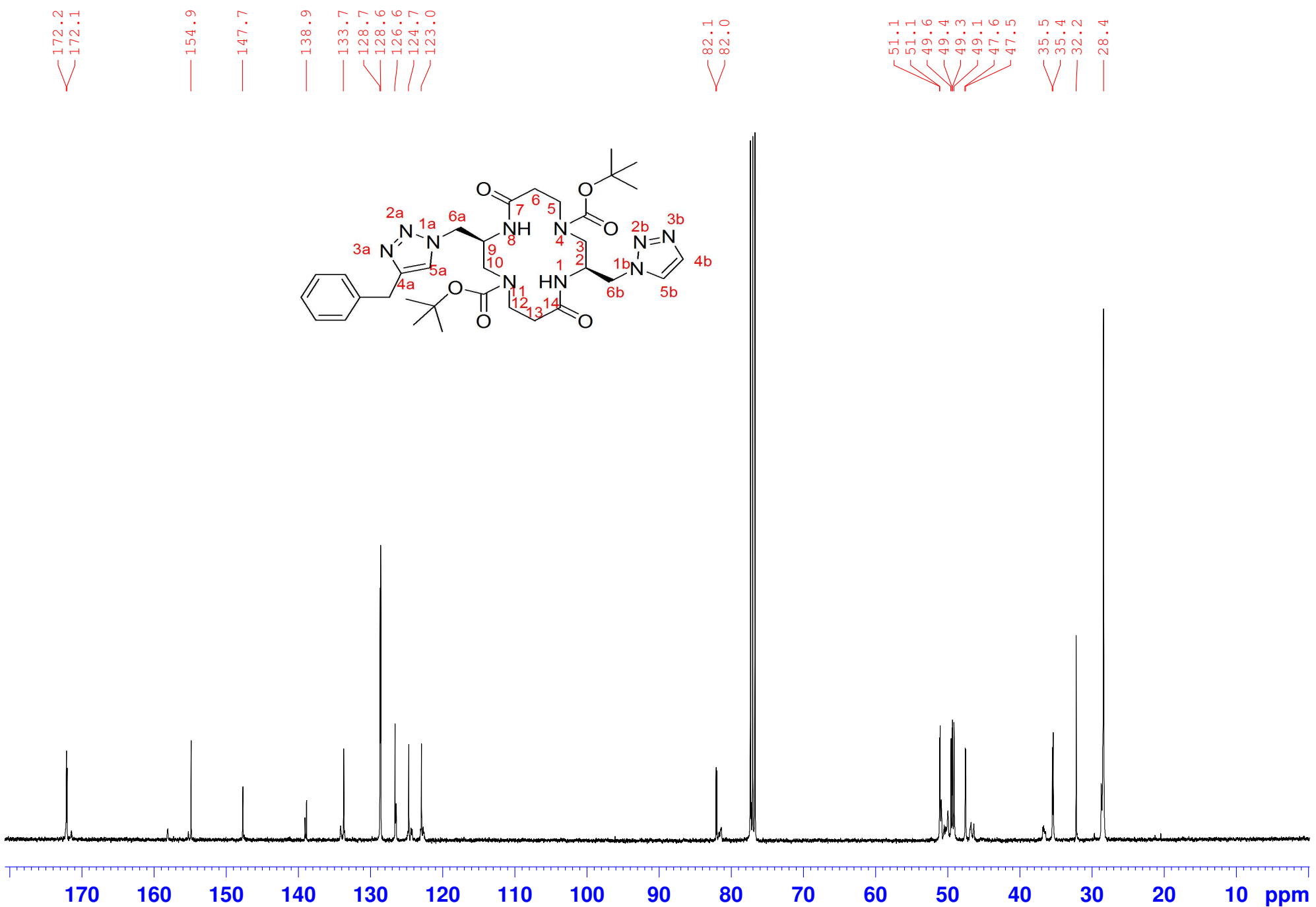
Compound 13, 100 MHz, CDCl₃



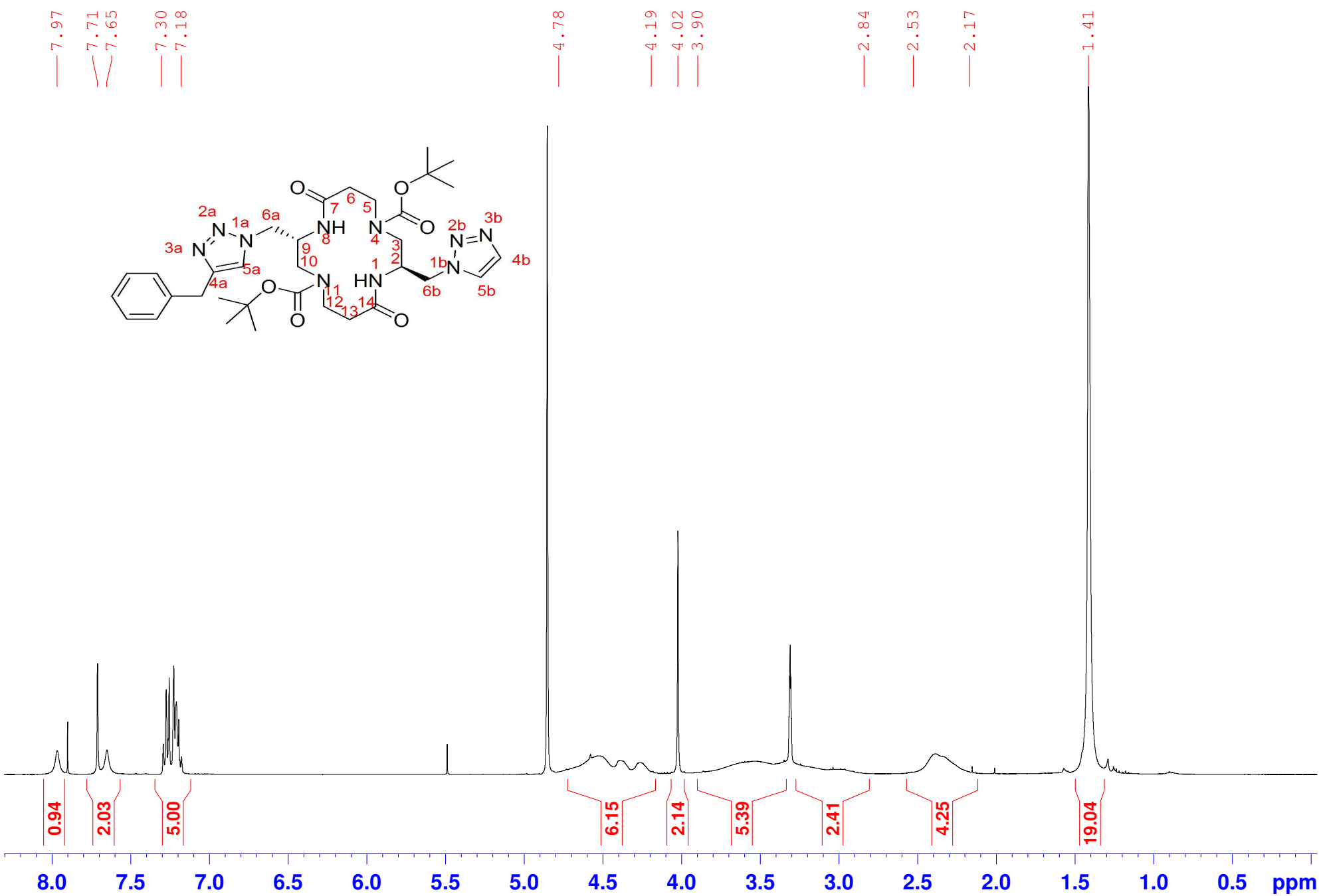
Compound 21, 400 MHz, CDCl₃



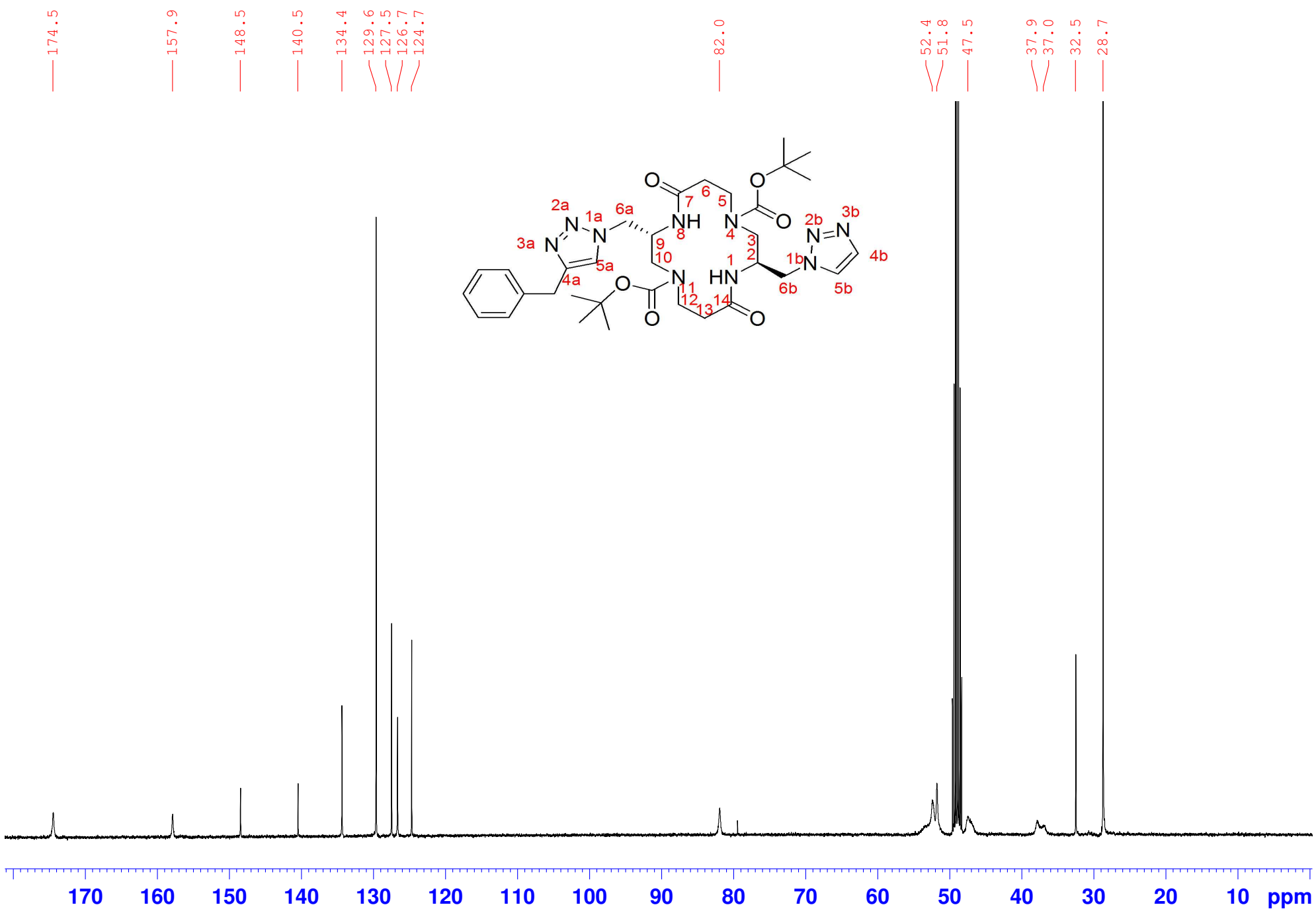
Compound 21, 100 MHz, CDCl₃



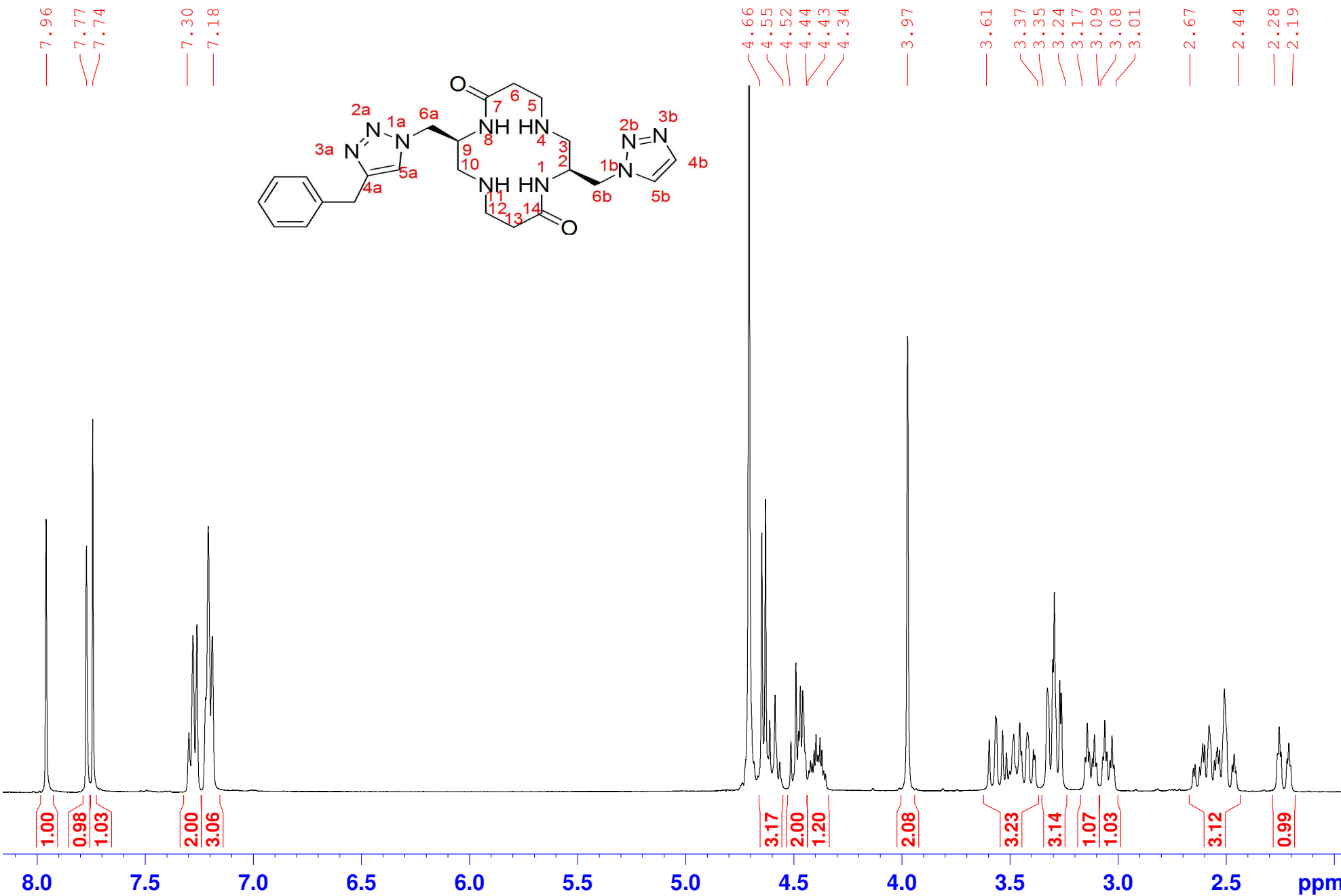
Compound 19, 400 MHz, CD₃OD



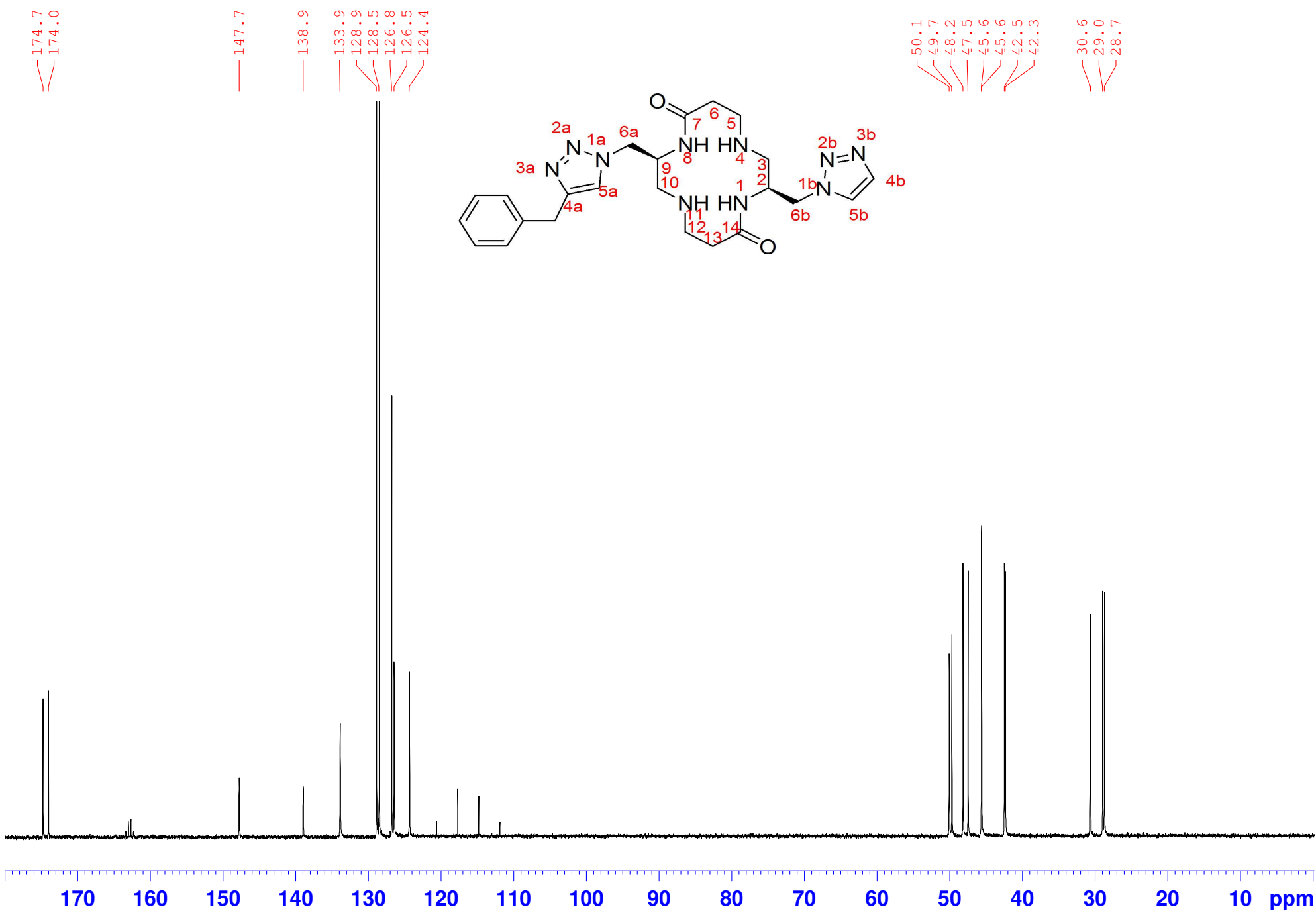
Compound 19, 100MHz, CD3OD



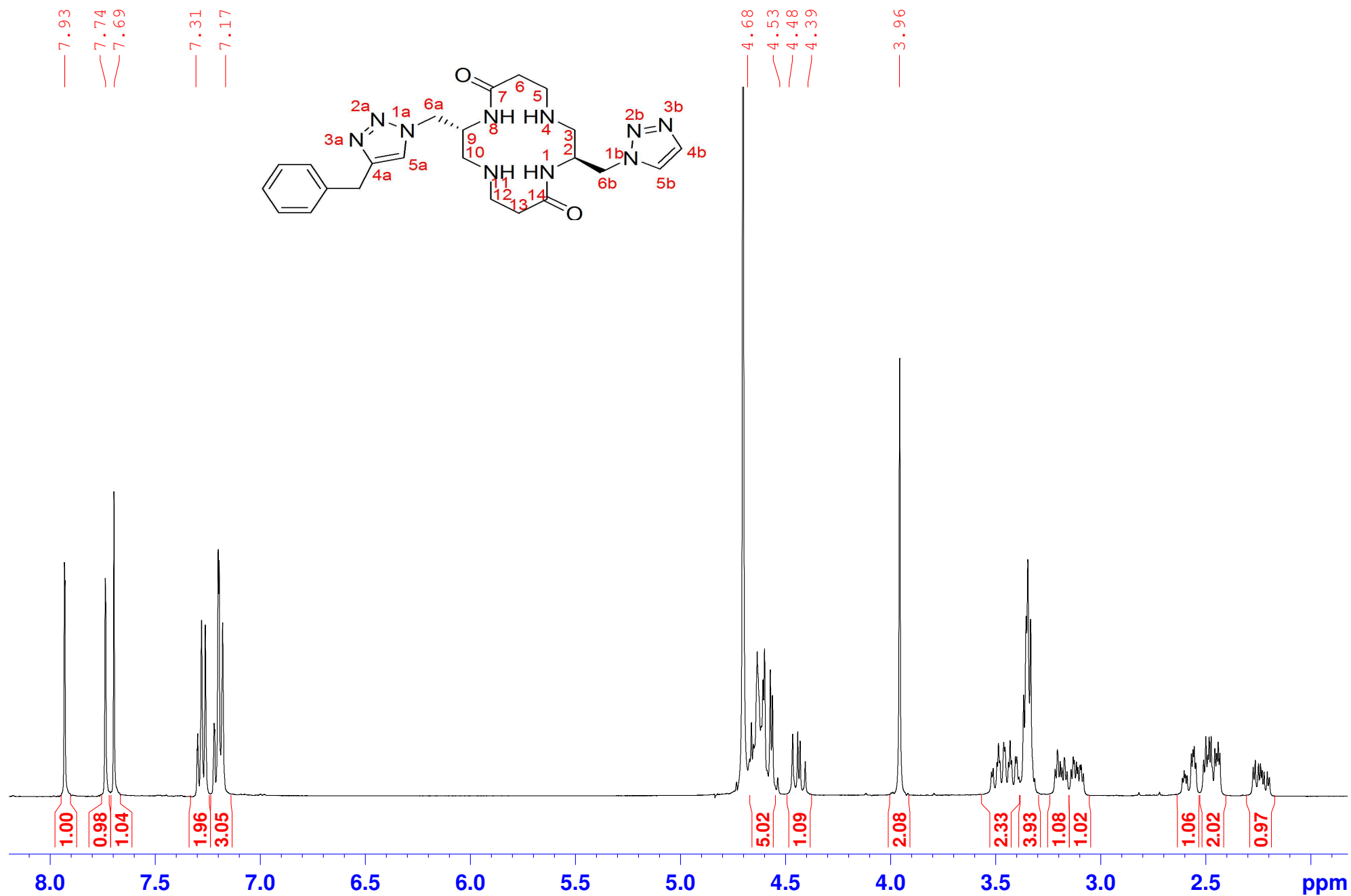
Compound 25, 400 MHz, D₂O



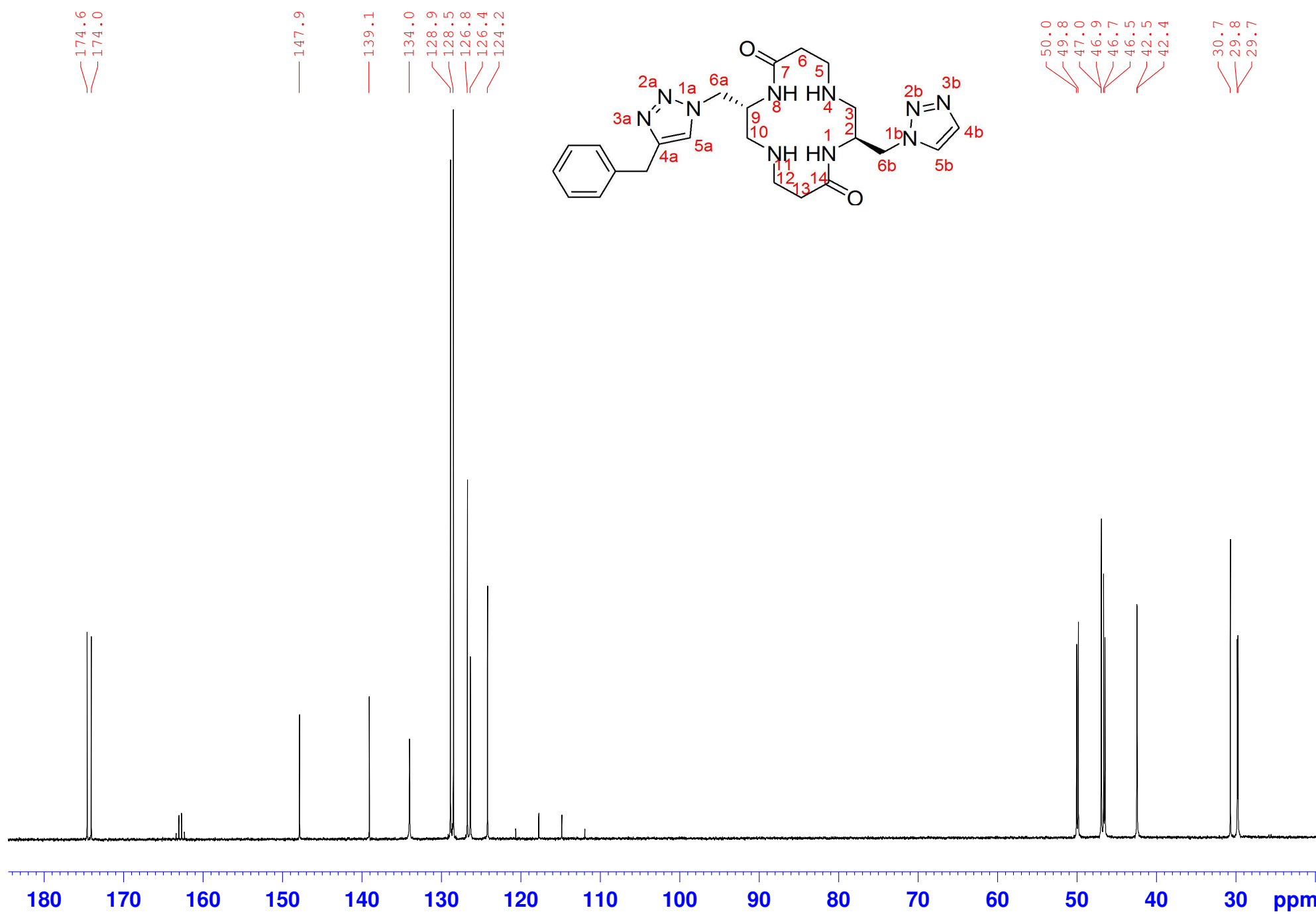
Compound 25, 100 MHz, D₂O



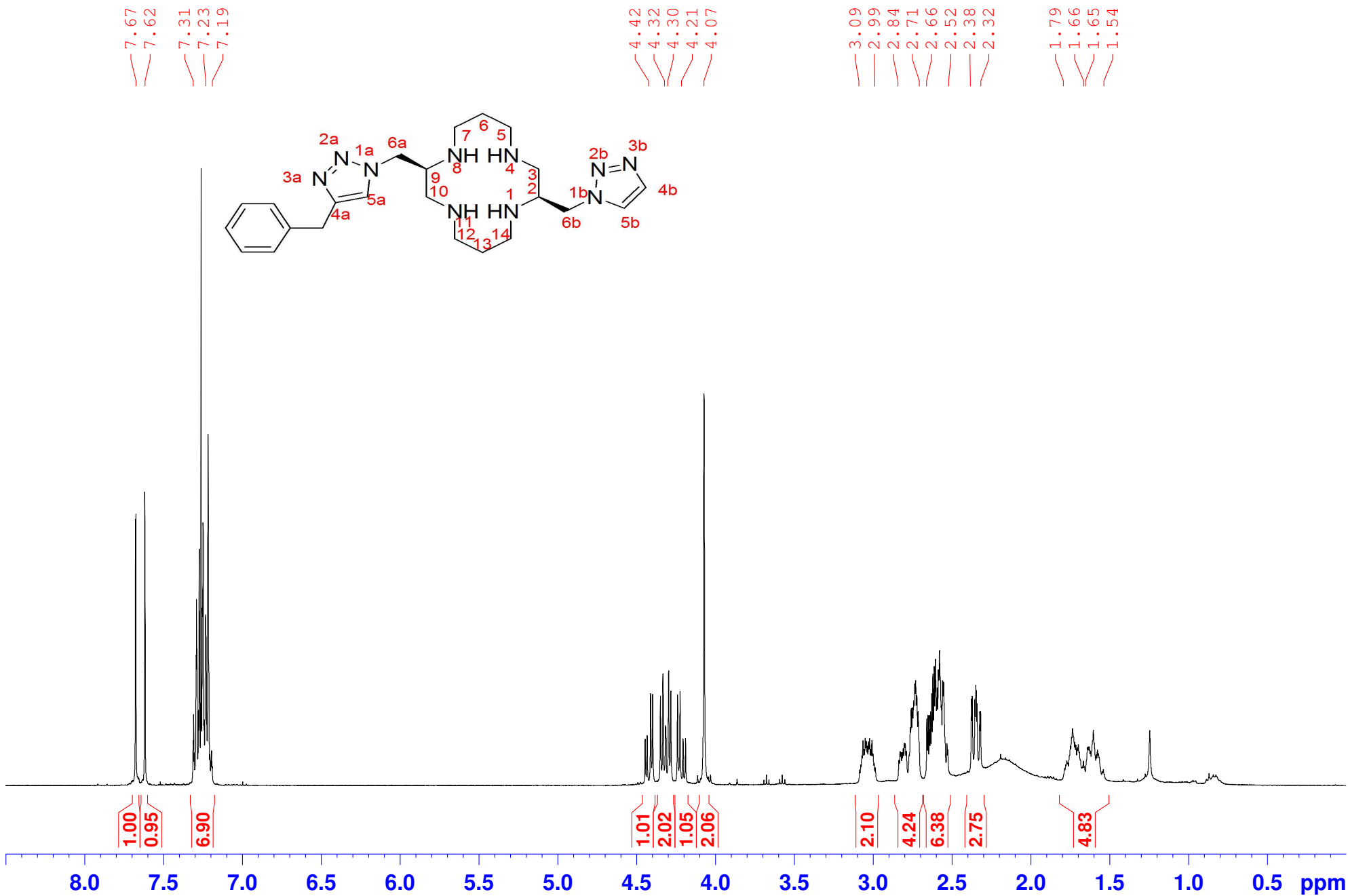
Compound 23, 400 MHz, D₂O



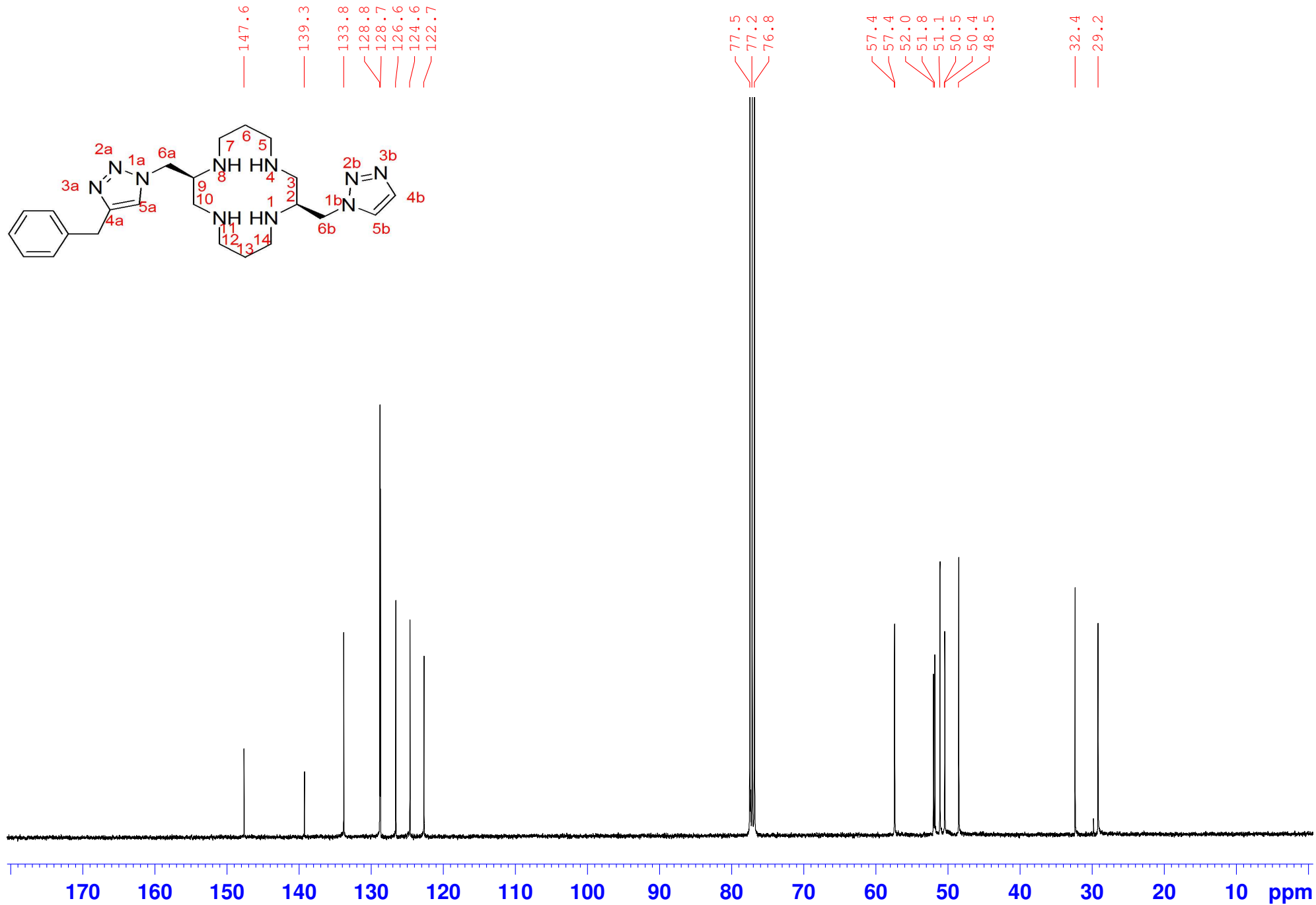
Compound 23, 100 MHz, D₂O



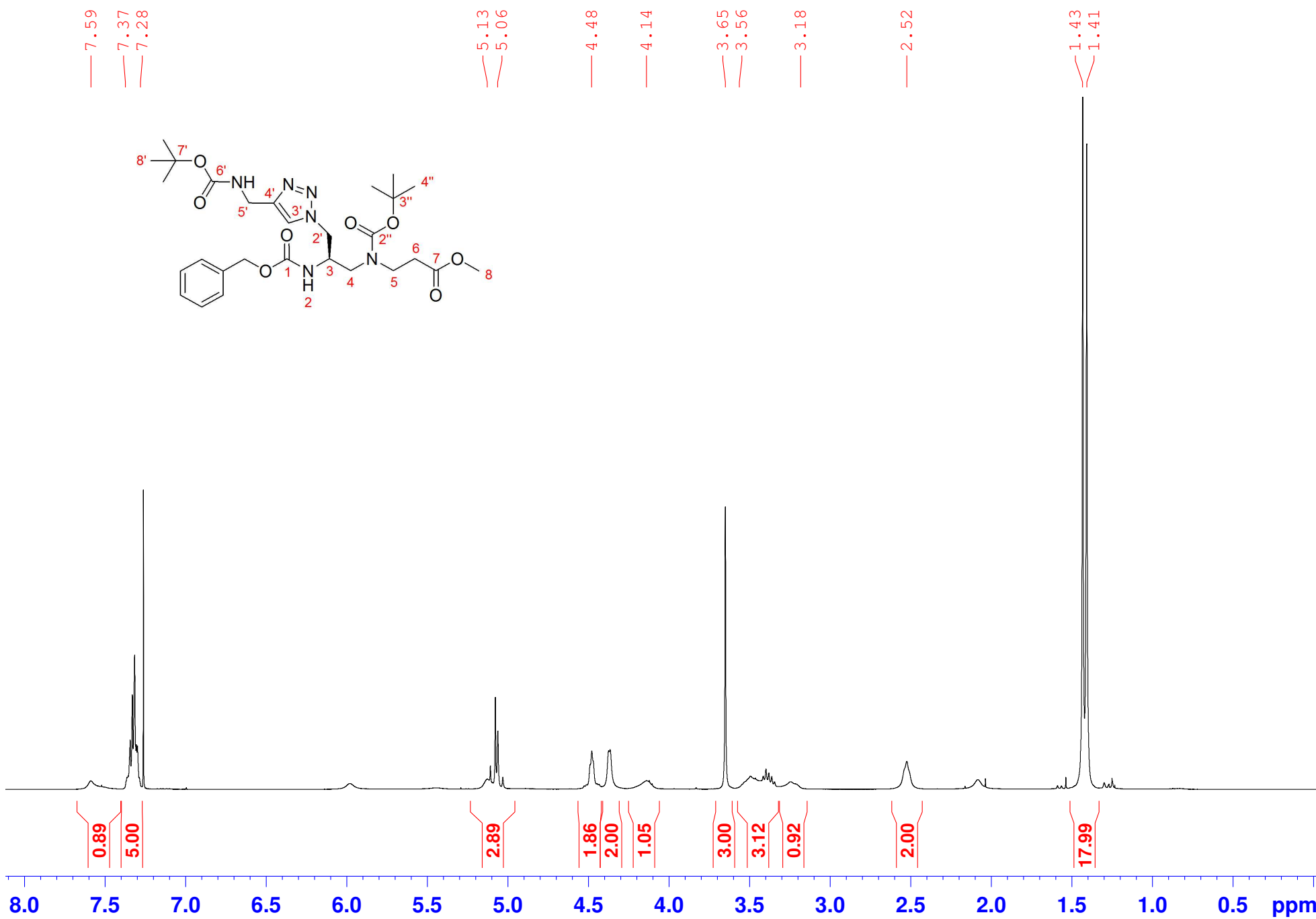
Compound 28, 400 MHz, CDCl₃



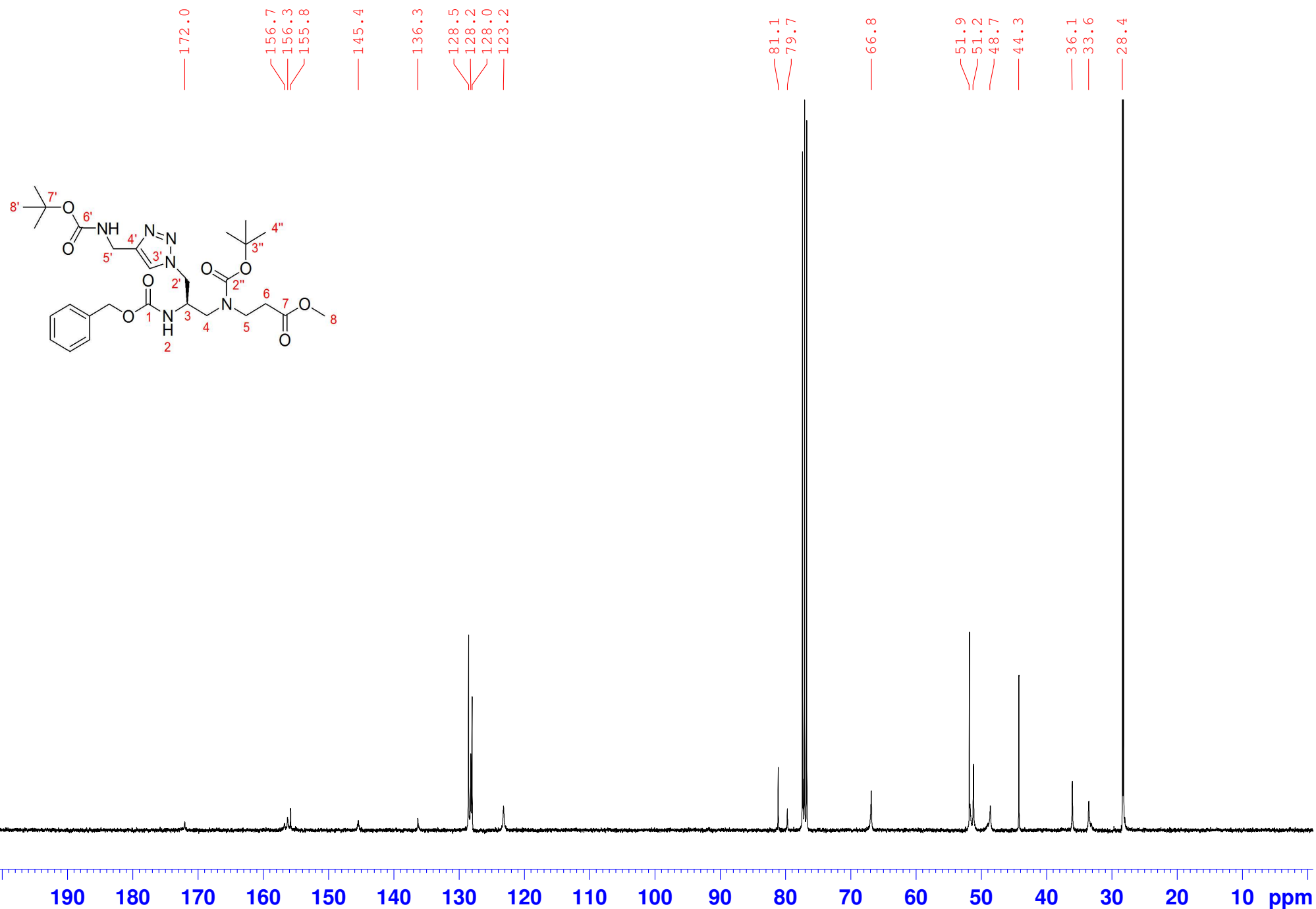
Compound 28, 100 MHz, CDCl₃



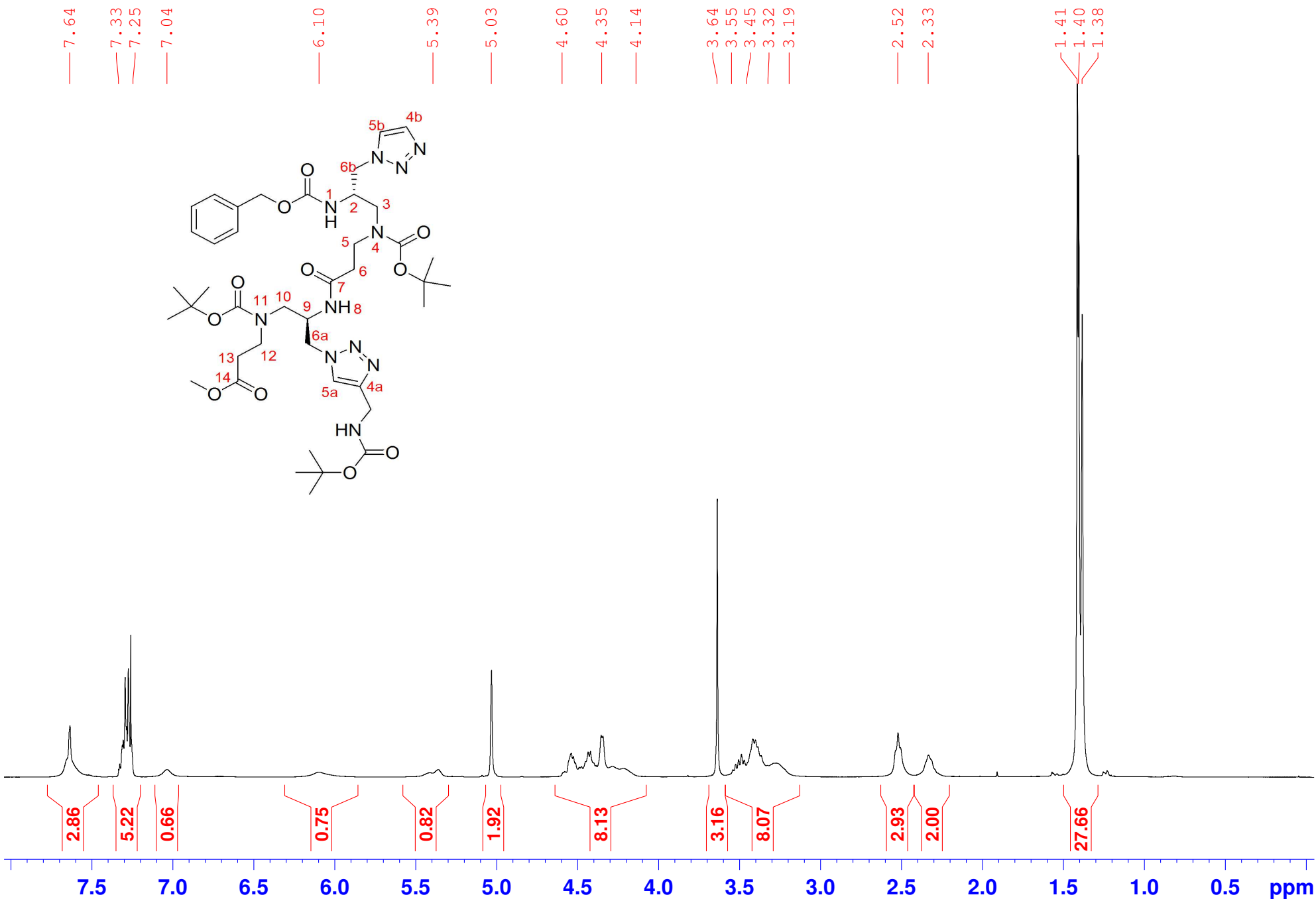
Compound 8, 400 MHz, CDCl₃



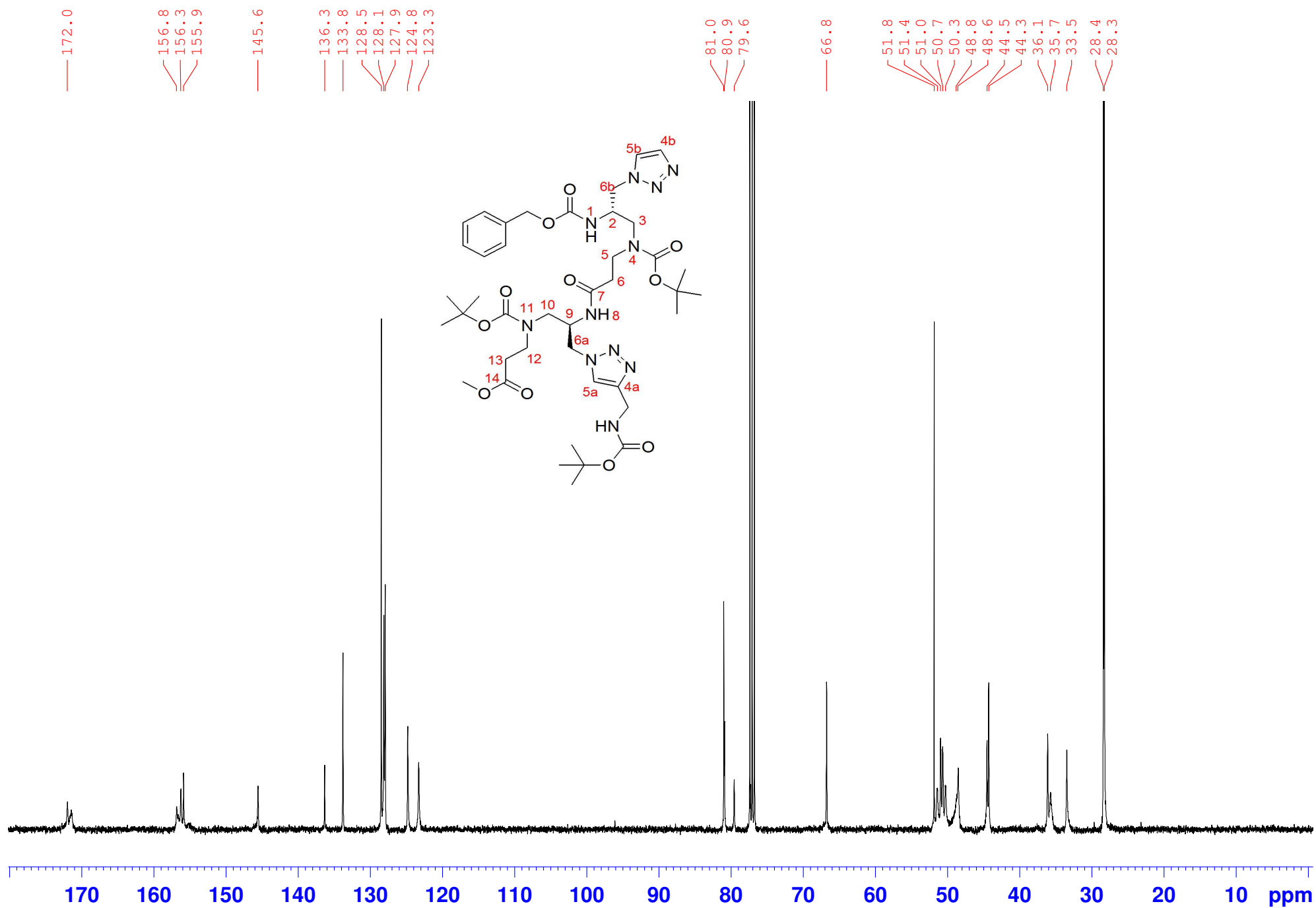
Compound 8, 100 MHz, CDCl₃



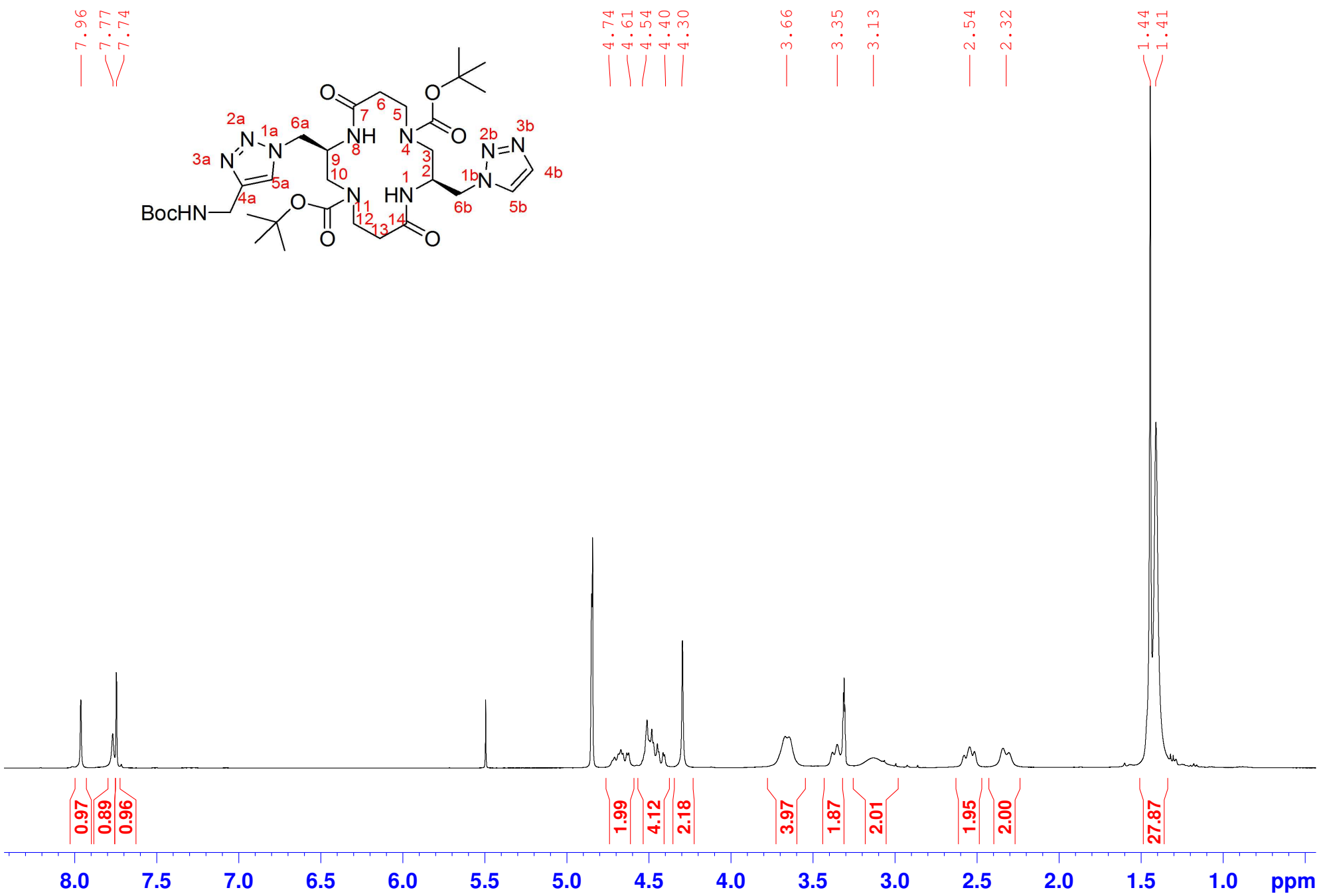
Compound 14, 400 MHz, CDCl₃



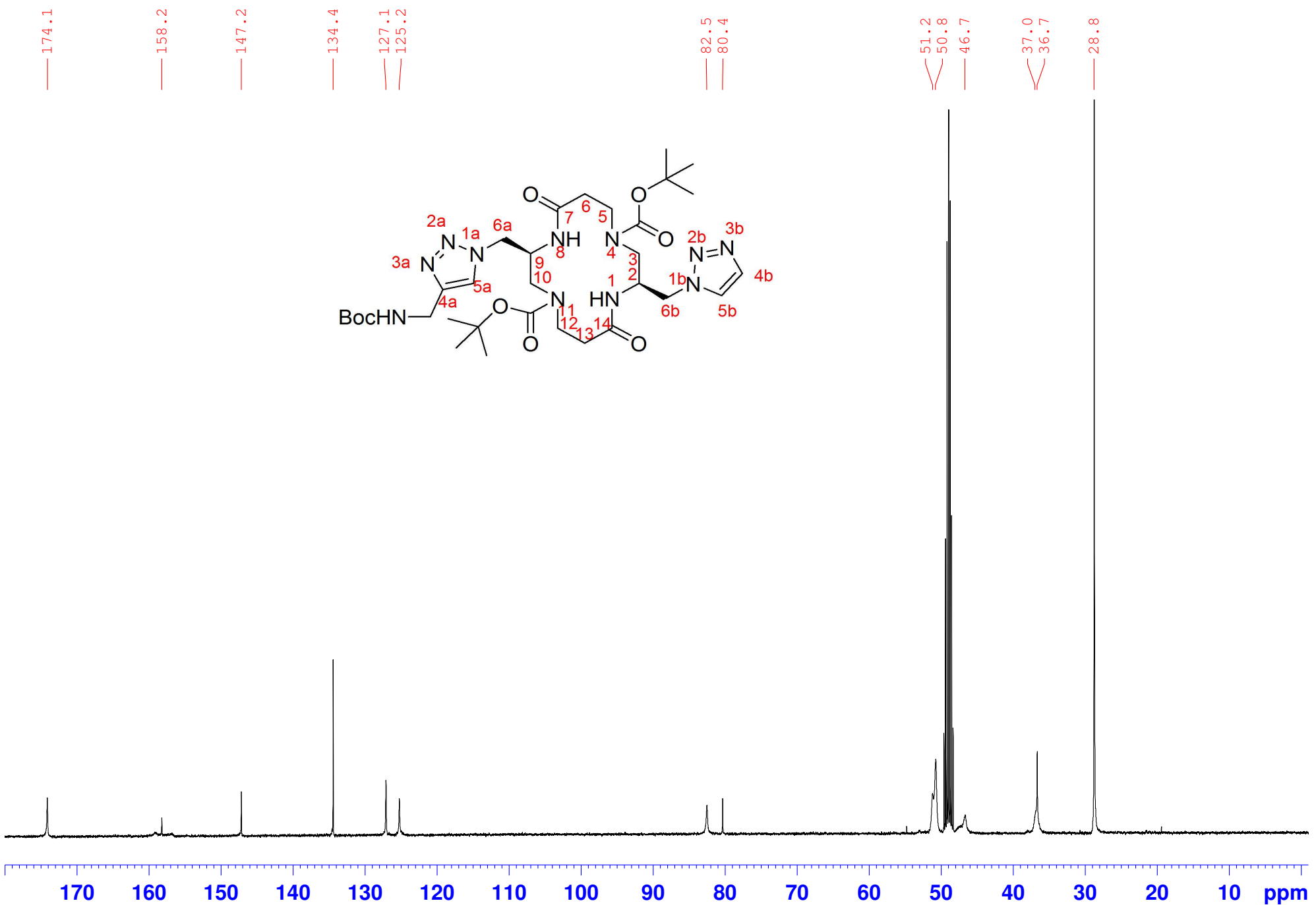
Compound 14, 62.5 MHz, CDCl₃



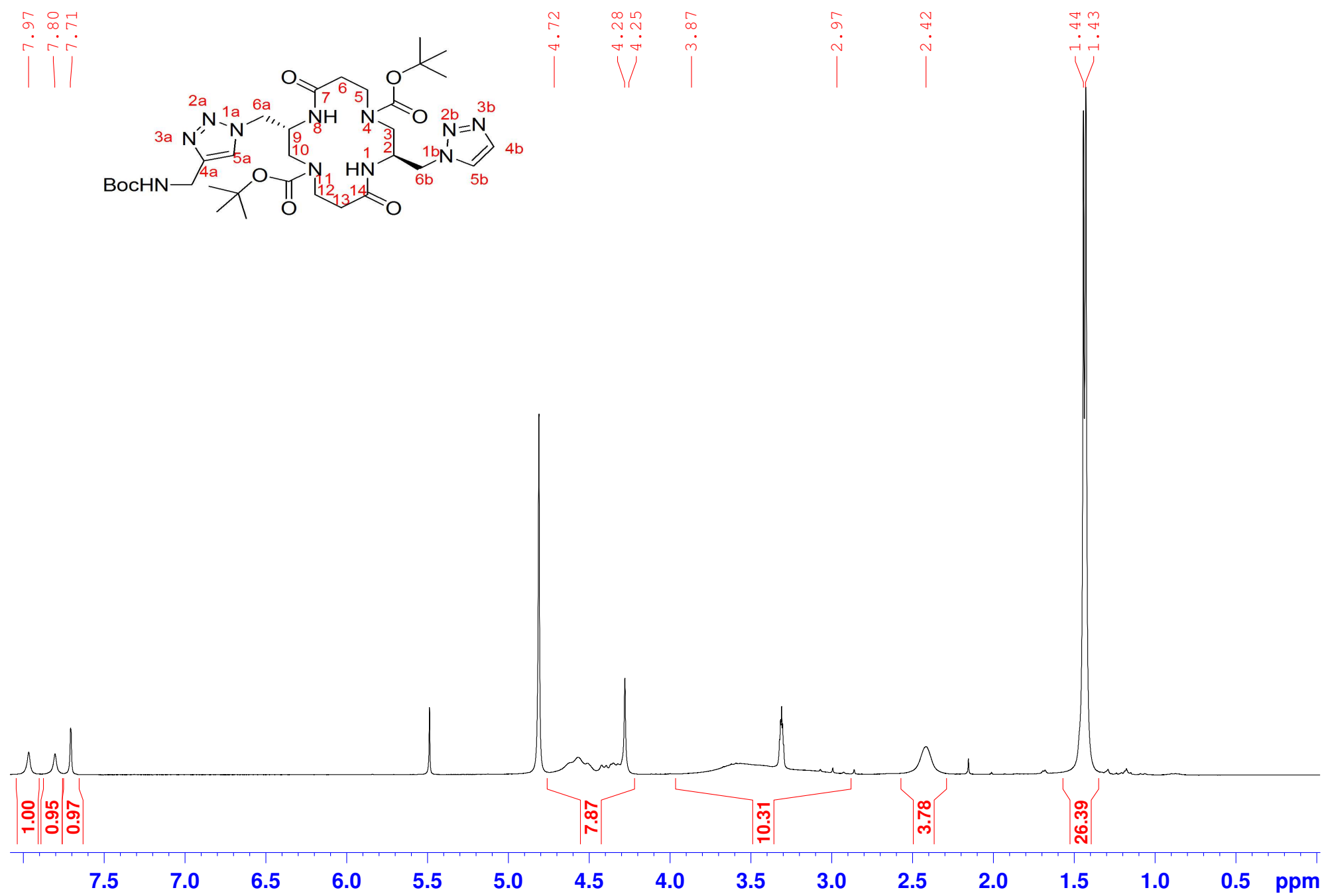
Compound 22, 250 MHz, CD₃OD



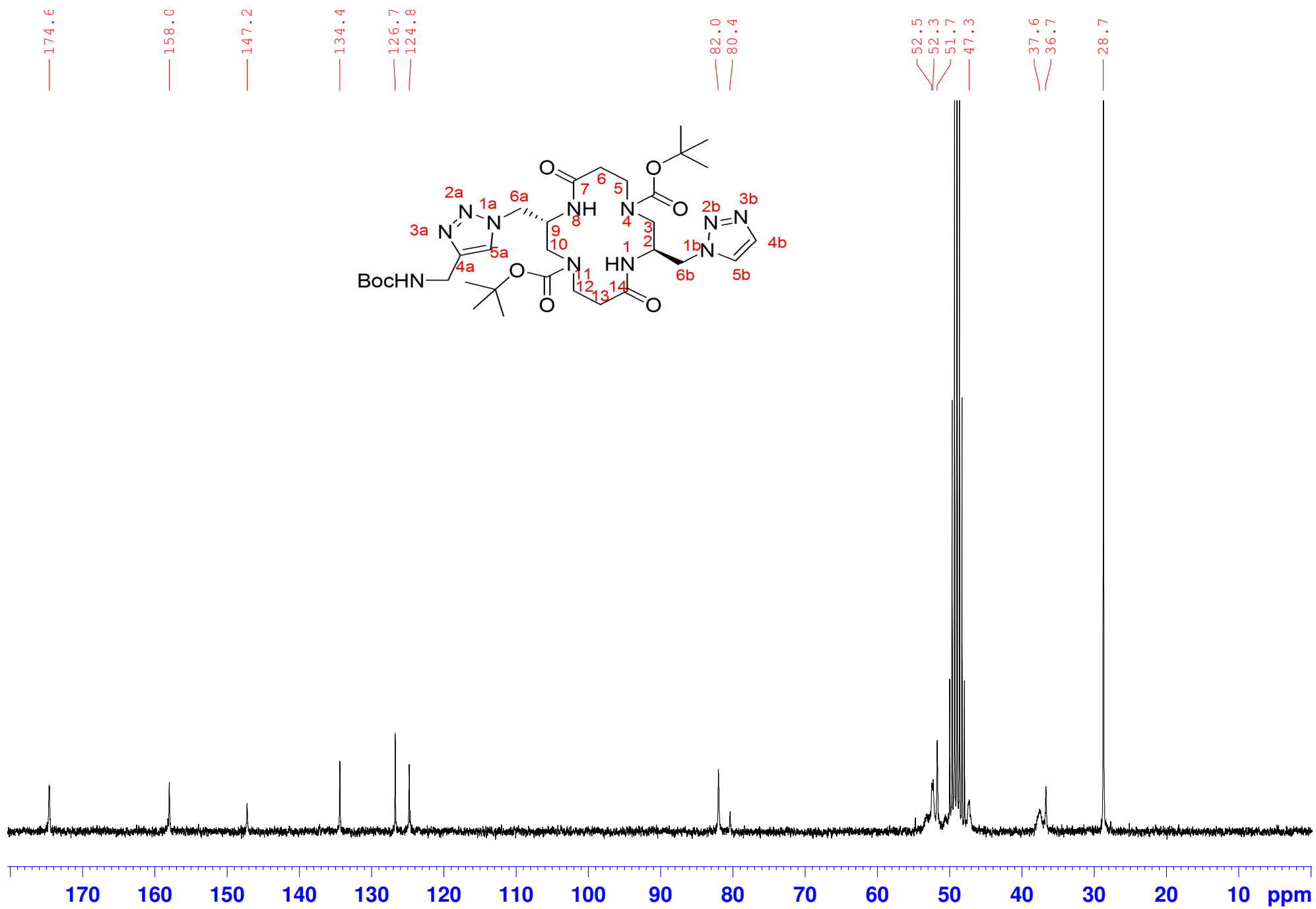
Compound 22, 62.5 MHz, CD₃OD



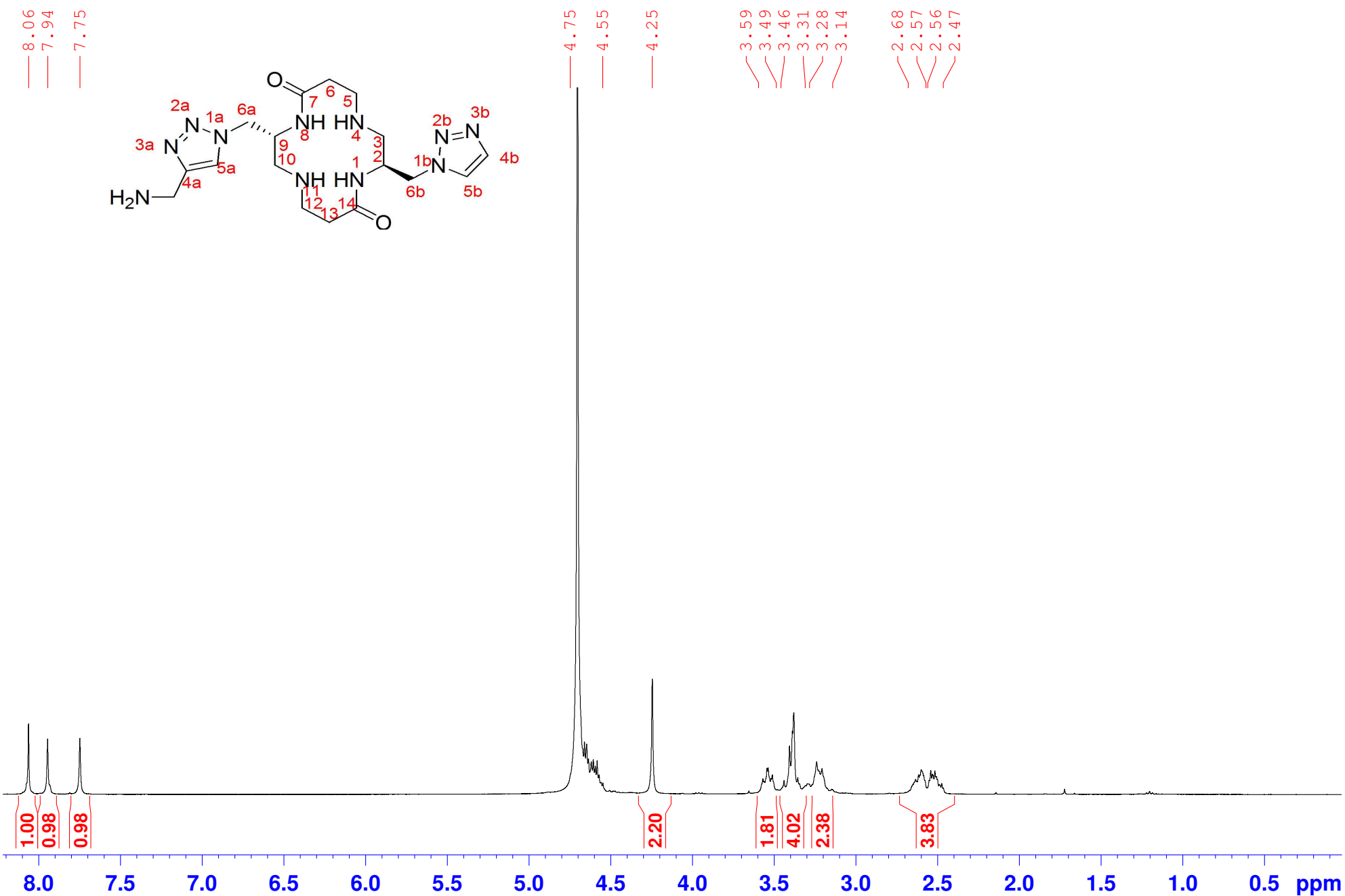
Compound 20, 250 MHz, CD₃OD



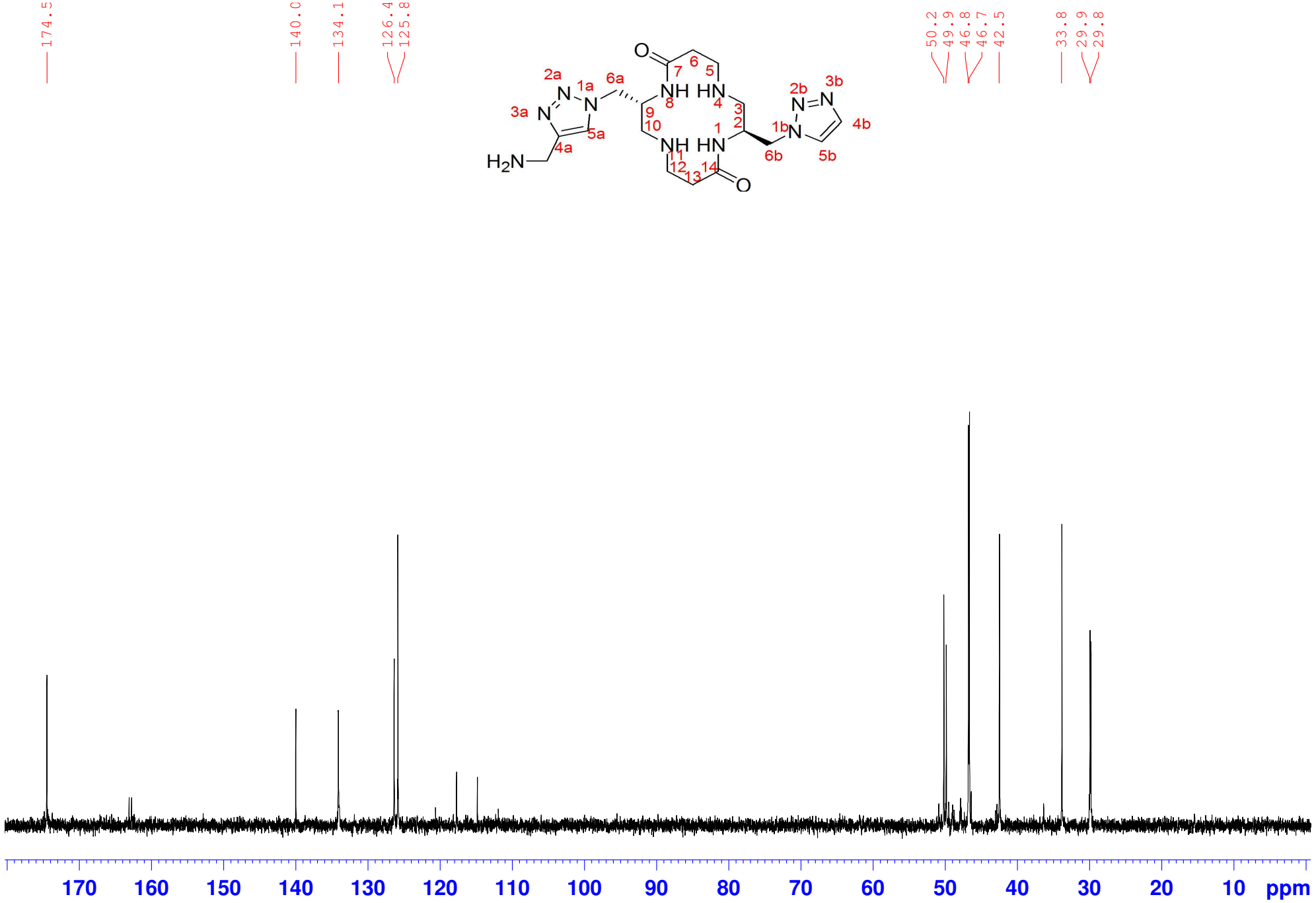
Compound 20, 62.5 MHz, CD₃OD



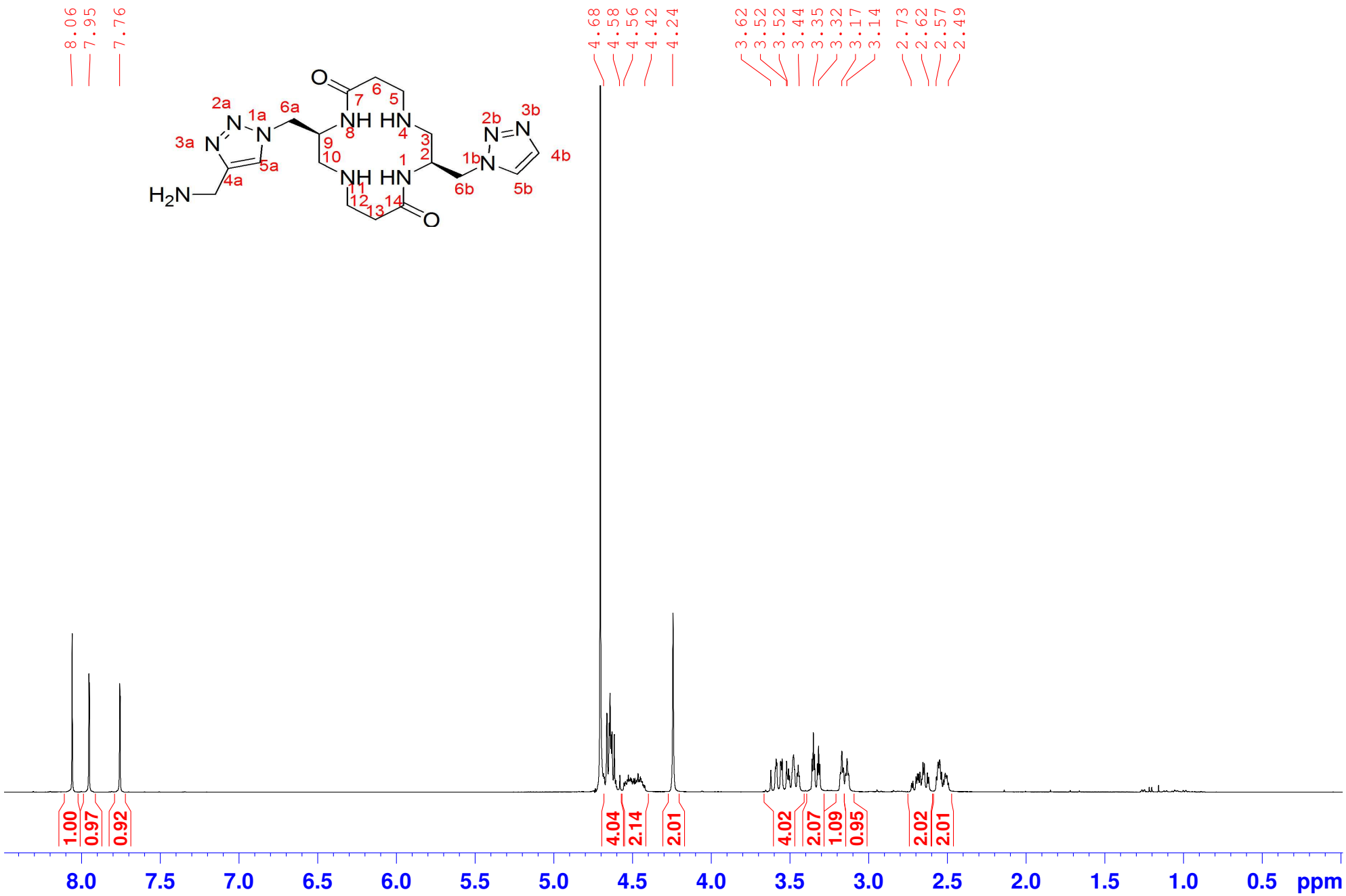
Compound 24, 250 MHz, D₂O



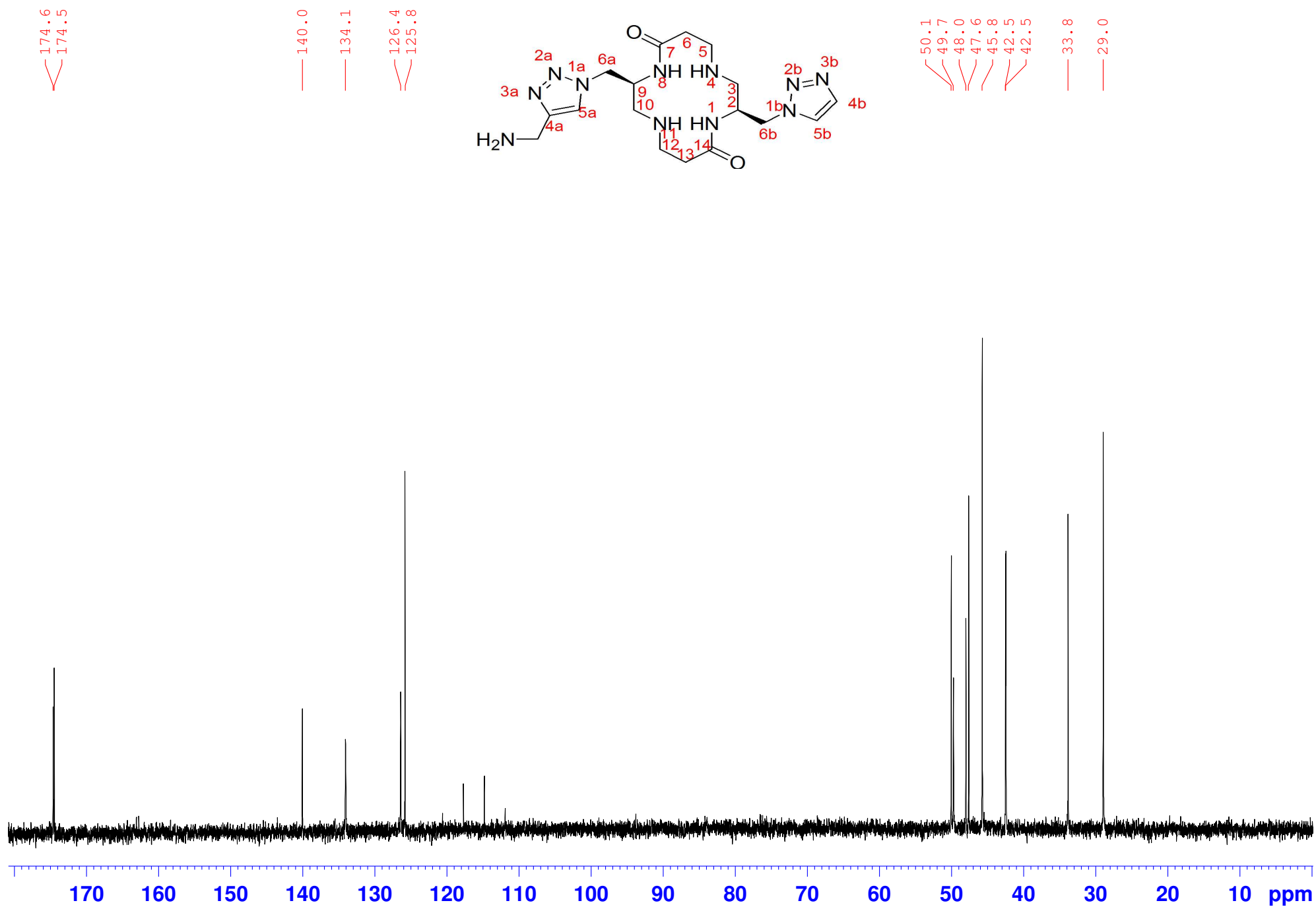
Compound 24, 62.5 MHz, D₂O



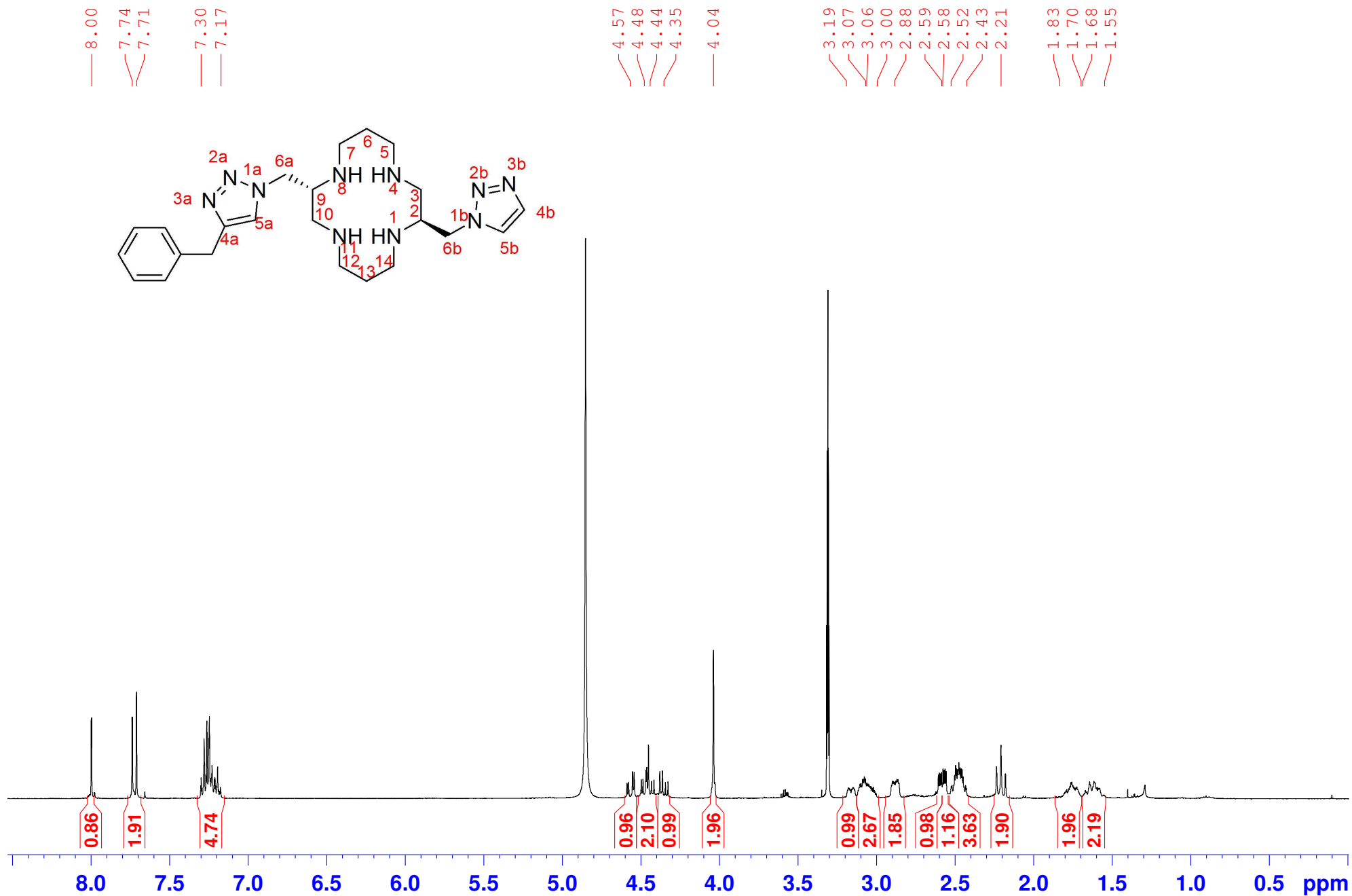
Compound 26, 400 MHz, D₂O



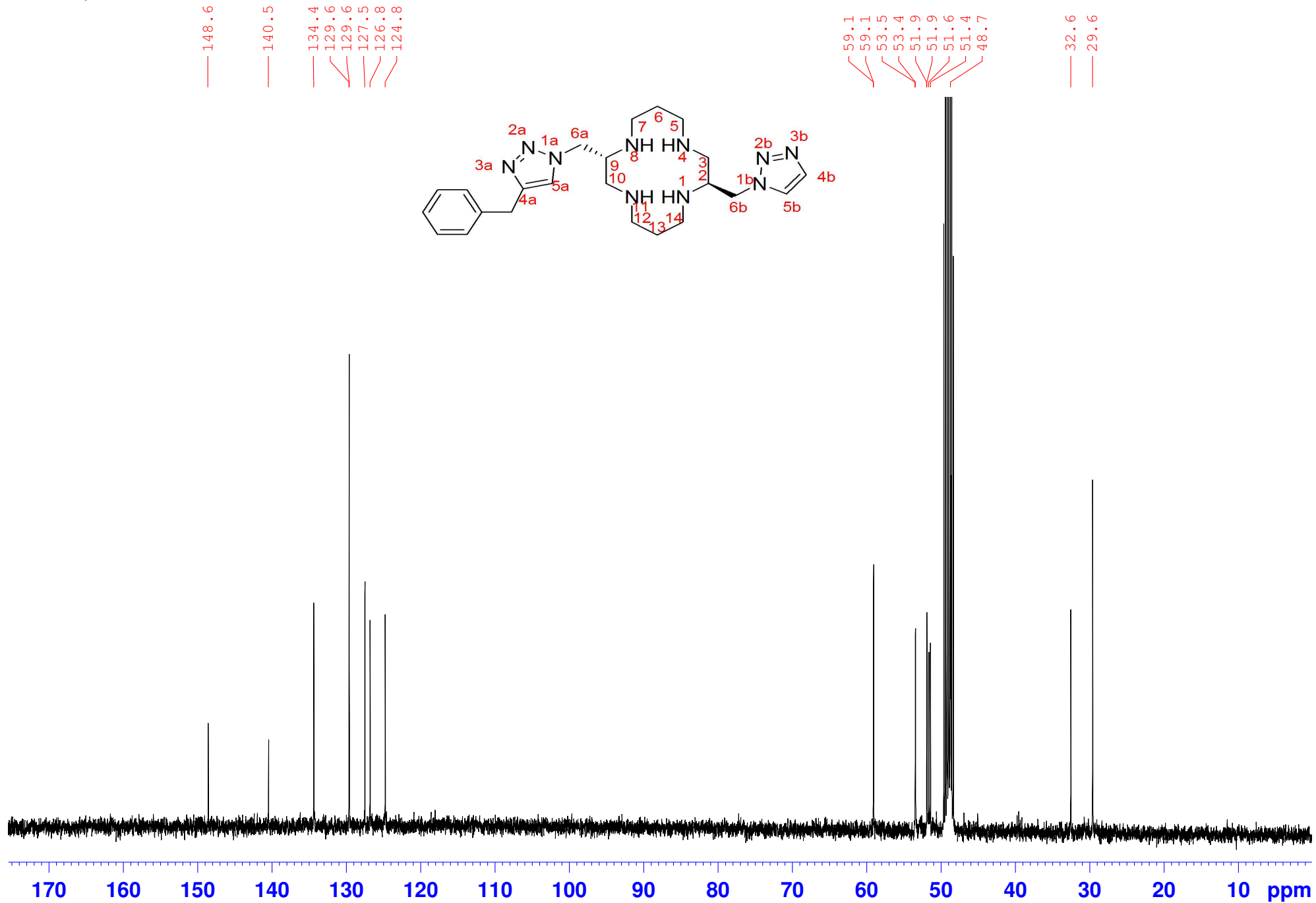
Compound 26, 100 MHz, D₂O



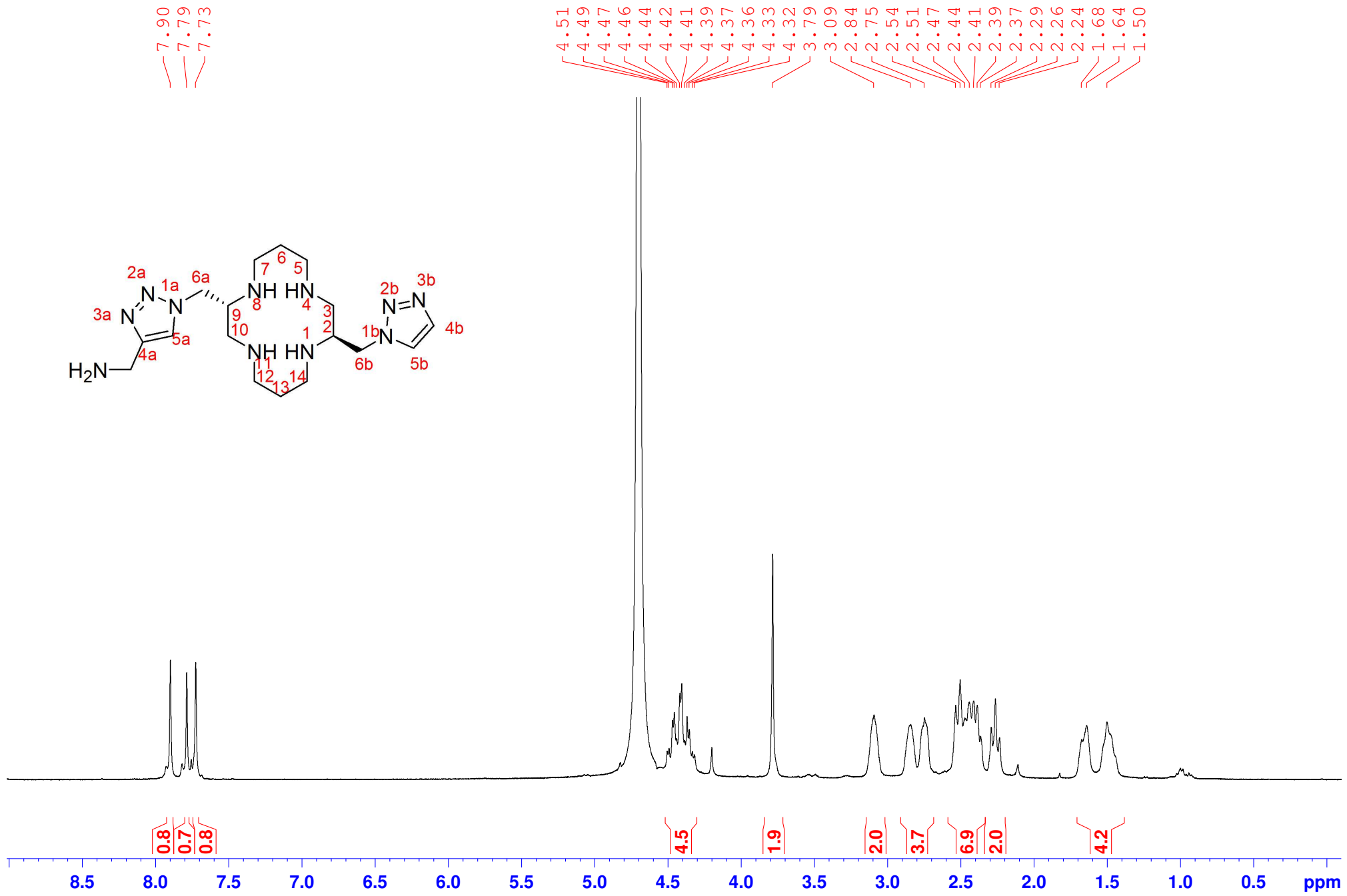
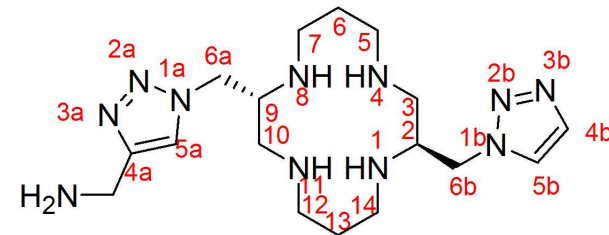
Compound 27, 400 MHz, CD₃OD



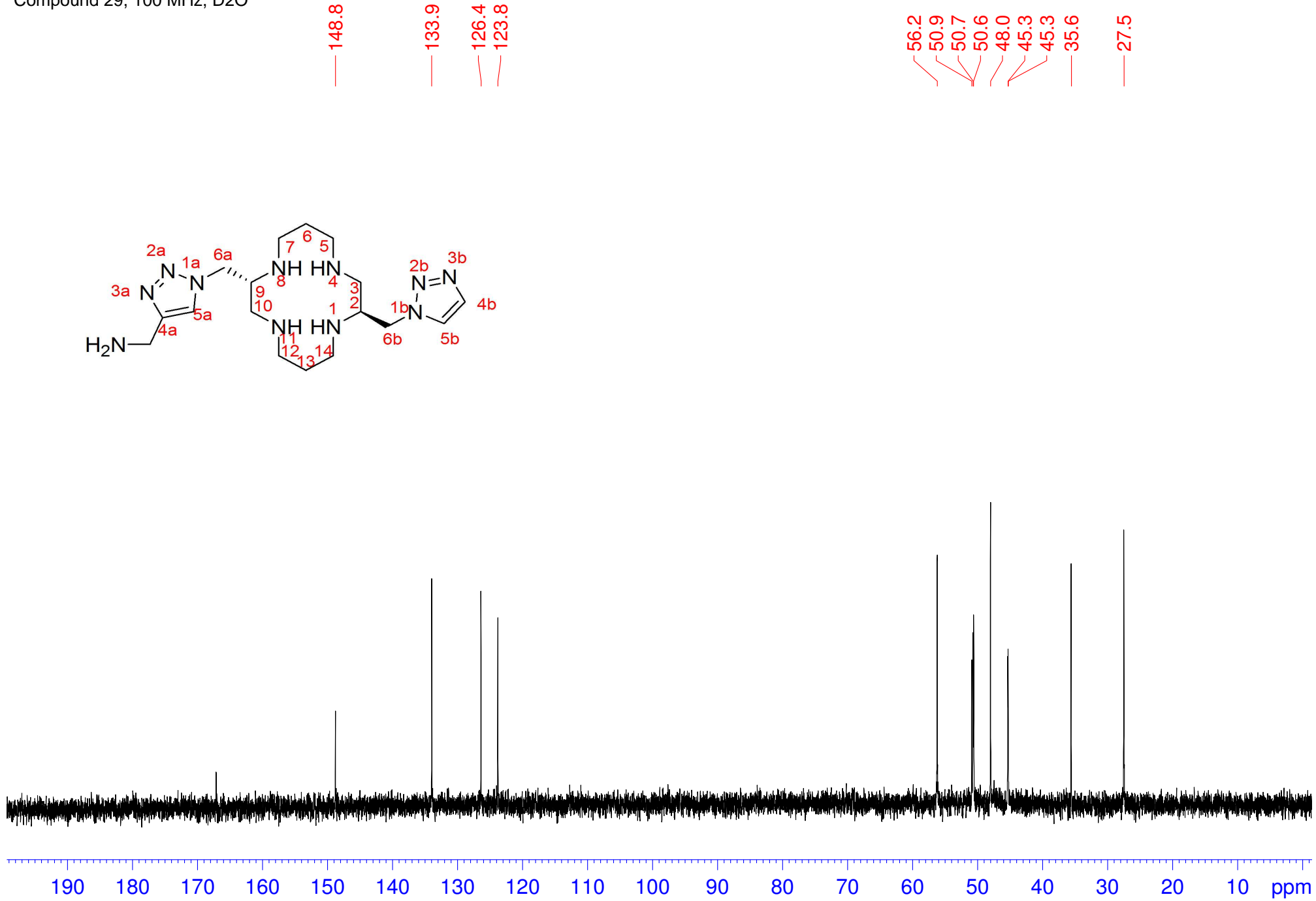
Compound 27, 100 MHz, CD₃OD



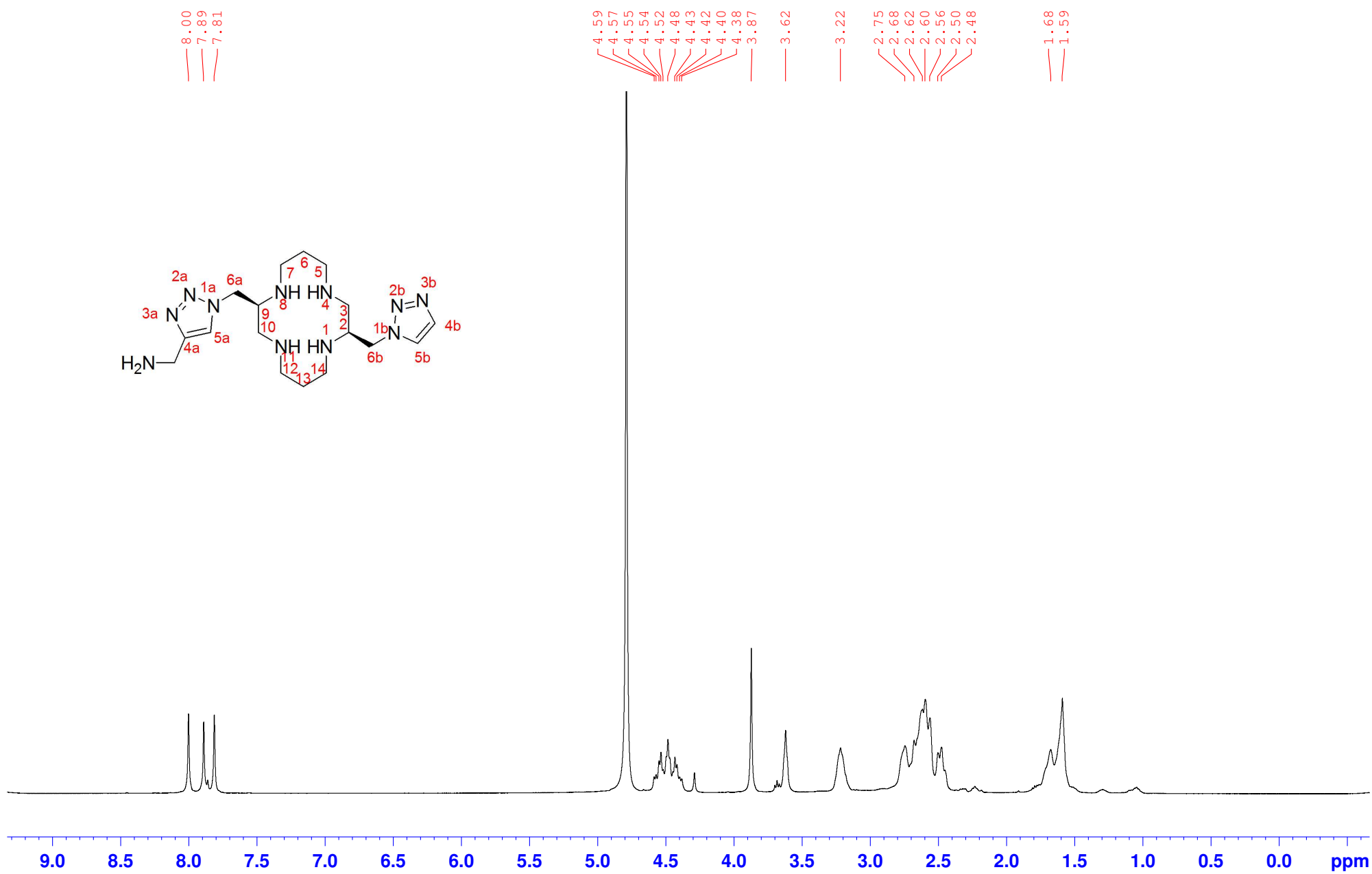
Compound 29, 400 MHz, D₂O



Compound 29, 100 MHz, D₂O



Compound 30, 400 MHz, D₂O



Compound 30, 100 MHz, D₂O

